Deep mutational scanning reveals tail anchor characteristics important for mitochondrial targeting

Abdurrahman Keskin, Emel Akdoğan, Cory D. Dunn*

Department of Molecular Biology and Genetics, Koç University, Sarıyer, İstanbul, 34450, Turkey

* Corresponding author

Mailing Address:

Dr. Cory Dunn
Koç Üniversitesi
Fen Fakultesi
Rumelifeneri Yolu
Sarıyer, İstanbul 34450
Turkey

Email: cdunn@ku.edu.tr
Phone: +90 212 338 1449
Fax: +90 212 338 1559

Running head: Comprehensive analysis of the Fis1 tail anchor

Keywords: mitochondrial targeting, mitochondrial protein import, membrane insertion, tail anchor, membrane protein biogenesis

ABSTRACT:

Proteins localized to mitochondria by a carboxyl-terminal tail anchor (TA) play roles in apoptosis, mitochondrial dynamics, and mitochondrial protein import. To reveal characteristics of TAs that are important for mitochondrial targeting, we examined the TA of the *Saccharomyces cerevisiae* Fis1 protein. We generated a library of Fis1p TA variants fused to the Gal4 transcription factor, then selected for mutations allowing Gal4 activity in the nucleus. Next-generation sequencing allowed quantification of TA variants in our mutant library both before and after selection for reduced TA targeting. High-throughput results were confirmed by further analysis of individual Fis1p TA mutants. Intriguingly, positively charged residues were more acceptable at several positions within the membrane-associated domain of the Fis1p TA than negatively charged residues. These findings provide strong, *in vivo* evidence that lysine and arginine can "snorkel" when associated with a lipid bilayer by placing their terminal charges at the membrane interface. Our work provides the first high-resolution analysis of an organelle targeting sequence by deep mutational scanning.

INTRODUCTION:

Proteins inserted within the mitochondrial outer membrane (OM) by a carboxyl-terminal tail anchor (TA) are important for programmed cell death, mitochondrial protein import, and the control of mitochondrial shape and number (Wattenberg and Lithgow, 2001). However, how proteins are targeted to mitochondria by TAs is not understood (Neupert, 2015; Lee et al., 2014). TA targeting seems to depend upon incompletely defined structural characteristics of the TA rather than a defined consensus sequence (Rapaport, 2003; Borgese et al., 2007). No components dedicated to TA insertion have been identified, and in fact, genetic and biochemical evidence suggest that spontaneous insertion of TAs might occur without the need for a translocation machinery (Kemper et al., 2008; Setoguchi et al., 2006). Such a mode of insertion stands in stark contrast with TA protein insertion into the endoplasmic reticulum (ER), which takes advantage of a conserved set of soluble proteins and membrane receptors (Johnson et al., 2013; Denic et al., 2013).

Genetic selection schemes using the organism *Saccharomyces cerevisiae* have been of high value in understanding how proteins reach their proper destination within the eukaryotic cell. During such studies, a protein required for survival under selective conditions can be mislocalized, and thereby made inactive, by a targeting sequence utilized by the transport process being studied. Next, mutations that allow return of this mistargeted protein to a region of the cell at which it can perform its function are recovered by selective conditions. *Trans* factors related to protein targeting are identified by standard genetic approaches. Alternatively, *cis* mutations in the targeting sequence are revealed, typically by Sanger sequencing of individual fusion construct clones. Most prominently, this genetic approach to studying protein targeting and transport has been important in understanding protein transit to and through the endomembrane system (Robinson et al., 1988; Deshaies and Schekman, 1987; Stirling et al., 1992). This approach has also been applied to the study of protein import and export at the mitochondrial inner membrane (He and Fox, 1999; Jensen et al., 1992; Maarse et al., 1992).

Even with the availability of powerful genetic strategies, a fine-grained analysis of any single eukaryotic protein targeting signal has been lacking. However, with the advent of next-generation sequencing, a more comprehensive analysis of protein targeting sequences is possible. In this study, we couple genetic selection to next-generation sequence analysis in order to reveal the structural and sequence characteristics important for localization of Fis1p, a protein targeted to the mitochondrial OM by its TA.

RESULTS:

Localization to the mitochondrial outer membrane via the Fis1 tail anchor prevents Gal4-mediated transcriptional activation

The TA of Fis1p is necessary (Mozdy et al., 2000) and sufficient (Förtsch et al., 2011; Kemper et al., 2008) for insertion of this polypeptide into the mitochondrial OM. Fis1p has been suggested to reach a final topology in the outer membrane in which the amino-terminal bulk of the protein faces the cytosol, a very short and positively charged carboxyl-terminus protrudes into the mitochondrial intermembrane space, and the two are connected by a membrane-anchoring domain (MAD) passing through the OM (Mozdy et al., 2000). In developing our selection for TA mutations that diminish Fis1p targeting, we reasoned that fusion of a transcription factor to Fis1p would lead to insertion within the mitochondrial OM and a lack of nuclear function (Figure 1A). Mutations within the TA of Fis1p that prevent effective membrane insertion would, however, presumably allow the linked transcription factor to enter the nucleus, promote expression of its targets, and allow survival under selective conditions. Toward this goal, we fused the Gal4 transcription factor to the amino-terminus of full-length Fis1p, since *S. cerevisiae* strains allowing titratable selection based upon Gal4p potency are readily available. We included GFP between the Gal4 and Fis1 moieties, but the signal was barely discernable during fluorescence microscopy, and we will not refer further to the presence of GFP when discussing Gal4-Fis1 constructs. Importantly, the Gal4-Fis1p fusion failed to complement the mitochondrial morphology defect of a *fis1Δ* mutant (A. Keskin, unpublished results), suggesting that our fusion protein cannot interact effectively with other mitochondrial division components that might potentially impede nuclear translocation of Gal4-Fis1p upon TA mutation.

To assess failed Gal4-Fis1p targeting to mitochondria, we specifically took advantage of Gal4-driven *HIS3* and *URA3* auxotrophic markers in MaV203, a strain commonly used for yeast-two-hybrid assays (Vidal et al., 1996b). Similar to cells containing an empty vector, Gal4p fused to Fis1p was unable to provide growth on medium lacking histidine and containing 20mM 3-aminotriazole (3-AT) to competitively inhibit any His3p produced independently of Gal4p activation (Durfee et al., 1993) (Figure 1B). However, the same Gal4-Fis1 polypeptide devoid of its TA [Gal4-Fis1(ΔTA)] provided ample proliferation on the same two selective media. This result indicated that our fusion protein could translocate to the nucleus upon TA disruption and that any potential lipid binding mediated by the cytosolic domain of Fis1p (Wells and Hill, 2011) will not prevent genetic assessment of TA functionality toward mitochondrial insertion.

Following validation of our experimental approach, we immediately sought mutations in the TA that would block targeting of Gal4-Fis1p to the mitochondrial OM by isolating colonies spontaneously arising on medium lacking uracil. Limited sequencing of the constructs encoding Gal4-Fis1p within these isolates revealed at least seven nonsense and 19 frameshift mutations out of a total of 32 plasmids analyzed. While these findings further validated the link between growth under selective conditions and damage to the Fis1p TA, continued encounters with

nonsense and frameshift mutations would not be greatly informative regarding the sequential or structural determinants important for TA targeting.

In the strain used for our selective scheme, a Ura$^+$ phenotype requires greater Gal4-dependent transcriptional activation than a His$^+$ phenotype (Vidal et al., 1996a). Therefore, we reasoned that initial selection of TA mutants based on a His$^+$ phenotype may provide informative mutations that weaken, but do not totally inhibit membrane association. We used mutagenic PCR to generate altered TAs within the context of a Gal4-Fis1 fusion protein. We then isolated four colonies that proliferated upon SMM-His medium containing 20mM 3-AT, yet exhibited diminished proliferation on SC-Ura medium when compared to cells expressing the Gal4-Fis1(ΔTA) polypeptide. Sanger sequencing of the region encoding the TA of Gal4-Fis1p within these colonies revealed one clone with a V145E mutation (amino acid numbering provided in this study will correspond to that of the unmodified, full-length Fis1p protein), two clones with a L139P mutation, and one clone with two mutations: L129P and V138A. Serial dilution assays (Figure 2A) confirmed that V145E and L139P provided a less than maximal, but still apparent Ura$^+$ phenotype, with the V145E mutant allowing more rapid proliferation on medium lacking uracil than the L139P mutant. The L129P/V138A mutant provided a His+ phenotype, but could not drive uracil prototrophy, suggesting a less severe localization defect than that exhibited by the other two mutant TAs. Interestingly, the V145E mutation falls within the MAD of the Fis1p TA, consistent with poor accommodation of a charged amino acid within this hydrophobic stretch of amino acids. Moreover, the Fis1p TA is predicted to be mostly alpha-helical in nature, so isolation of the potentially helix-disrupting L139P replacement by selection may indicate a need for TA helicity for mitochondrial targeting.

We then verified that these mutations presumably disrupting TA targeting are not isolated merely as a consequence of the Gal4p-based selection system that we had applied. Toward this goal, we took advantage of the Pdr1 transcription factor, which promotes resistance to several drugs(Prasad and Goffeau, 2012; Meyers et al., 1992). The *PDR1-249* allele encodes a hyperactive Pdr1p known to provide cycloheximide (CHX) resistance (Mutlu et al., 2014). Fusion of the hyperactive Pdr1-249 protein to the unmutated Fis1p TA did not allow CHX resistance (Figure S1). However, addition of the V145E mutation to the TA in this fusion protein did permit CHX resistance, presumably as Pdr1-249p entered the nucleus to activate its targets. These findings demonstrate that mutations recovered using our Gal4p-based scheme are unlikely to be related to the use of any specific transcription factor.

Transcription driven by Gal4-Fis1p indirectly reports on TA targeting to mitochondria and may be affected by mutant stability, ability of the fusion protein to translocate to the nucleus, or other events unrelated to normal TA localization. To further examine whether isolated TA mutations affect mitochondrial OM targeting, we linked wild-type (WT) or mutant Fis1p TAs to the carboxyl-terminus of mCherry. To assess mitochondrial localization of these fusion proteins, mitochondria were specifically labelled with GFP targeted to mitochondria by the presequence of the Cox4 protein (Sesaki and Jensen, 1999). Importantly, the TA of Fis1p lacks

information required for mediating mitochondrial fragmentation (Habib et al., 2003), indicating that the localization of these constructs should not be influenced by interaction partners of full-length, inserted Fis1p.

The location of mCherry fused to Fis1p TAs faithfully recapitulated our genetic findings. V145E and L139P mutations in the Fis1p TA led to very substantial cytosolic localization of mCherry (Figure 2B). Moreover, the L129P/V138A TA, consistent with its weaker activation of Gal4 targets in our selection system, provided still discernable mitochondrial localization of the mCherry signal, but cytosolic levels of this mutant fusion protein appeared increased. These results suggest that, in general, our genetic approach is likely to accurately report upon the ability of the Fis1p TA to moor proteins to the mitochondrial outer membrane.

Deep mutational scanning uncovers determinants of Fis1p tail-anchor targeting

Buoyed by our initial isolation of TA mutations affecting mitochondrial localization, we decided to take a more global approach to the analysis of the Fis1p TA. Using degenerate primers and recombination-based cloning in *S. cerevisiae*, we sought to generate a library consisting of all possible codons at every one of 27 amino acid positions within the TA of Gal4-Fis1p. We then allowed the pool of cells containing mutant TAs to divide four times under six possible culture conditions: no specific selection for *HIS3* or *URA3* reporter activation (SC-Trp, selecting only for plasmid maintenance), selection for *HIS3* activation at different 3-AT concentrations (SMM-Trp-His +0, 5, 10, or 20mM 3-AT), or selection for *URA3* activation (SC-Ura). Plasmid DNA was isolated from each pool of mutants, and TA coding sequences were amplified and subjected to next-generation sequencing. We then focused our analysis only on those clones within our pools that carried zero or one amino acid changes.

While all potential replacement mutations could not be detected within our starting library (Figure S2), and some biases did exist at each TA position, most potential amino acid mutations were represented within our pool. 98.9% of potential amino acid replacements were identified in the starting pool cultured in SC-Trp, and 95.9% of TAs with single mutations were represented by at least 10 counts. Quantification of counts from all samples can be found in Table S1. When comparing the mutant pool cultured in SC-Trp with selection in SMM-Trp-His without added 3-AT, there was no appreciable difference in the relative abundance of most mutants, including truncation mutations expected to totally prevent mitochondrial targeting of Gal4-Fis1p (Figure S3A). Such a result is consistent with 'leaky' expression of *HIS3* independent of Gal4-driven activation (Durfee et al., 1993). However, upon addition of 3-AT at concentrations of 5mM (Figure S3B), 10mM (Figure S3C), or 20mM (Figure 3) to medium lacking histidine, there were substantial shifts in the composition of the mutant pools toward specific amino acids, prompting further experiments that we describe below. The pool cultured in SC-Ura medium showed very strong selection for nonsense mutations within the TA (Figure S3D), but less prominent biases among amino acids. When considering our initial findings, in which recovery of uracil prototrophs in our genetic scheme led to a high recovery of frameshift and nonsense mutations, assessment of *HIS3*

activation seems more informative regarding determinants of Fis1p TA targeting than competition assays performed in the more strongly selective uracil dropout medium.

Independently of the primary amino acid sequence, the specific codons used to direct synthesis of a protein can affect that polypeptide's translation rate and folding (Yu et al., 2015). Although TAs shorter than the ribosome exit tunnel, which is 30 to 40 residues in length (Voss et al., 2006), must certainly be inserted post-translationally, we also examined enrichment of specific codons following selection for Gal4-Fis1p presence in the nucleus. However, this approach did not provide notable evidence of a role for specific codons in directing localization of the Fis1p TA (Figure S4). While the data are more 'noisy' due to a lack of representation of certain codons at each position, codons encoding the same amino acid generally acted in concert with one another within our selection scheme, placing our focus on the amino acid sequence of library variants rather than on codon sequence.

Proline is not acceptable at many locations within the Fis1p tail anchor

Consistent with previous analyses of tail-anchored mitochondrial proteins, there is apparently no strict requirement for a single, specific amino acid at any given position within the TA (Rapaport, 2003; Borgese et al., 2007); most amino acid replacements within the WT TA sequence fail to lead to selectable reporter activation (Figure 3). We focused our subsequent analysis on general characteristics of the TA that might be important for mitochondrial OM targeting.

The recovery of the L139P mutation during preliminary selection for Fis1p TA mutations indicated that proline may not be acceptable within the hydrophobic core of the Fis1p TA. Our deep mutational scan of the Fis1p TA in SMM-Trp-His+20mM 3-AT (Figure 3) also strongly indicated that proline insertion across many positions disrupted mitochondrial TA localization. When focusing specifically upon those mutants that were in the top 75% most commonly counted variants in the starting pool (>126 counts) and enriched at least four fold in SMM-Trp-His + 20mM 3-AT, 12 of 33 missense mutations within this set were proline replacements (Figure 4), further indicating failure of TA targeting following placement of proline at many TA positions.

Subsequently, we carried out directed experiments to further examine poor accommodation of proline within the Fis1p TA. We further studied the L139P mutant initially isolated during selection for Fis1p TA targeting mutants, and we also examined four additional proline replacements within Gal4-Fis1p. All proline replacement mutations were then tested individually for Gal4-driven reporter activation. V134P, L139P, and A140P mutations, consistent with our larger scale analysis (Figure 3 or Figure 4), provided ample proliferation on medium selective for *HIS3* activation (Figure 5A). Only the A144P mutant behaved differently during pool analysis and when tested individually on selective medium, at least raising the possibility that not every result obtained by bulk analysis might be recapitulated with individually constructed clones. We noted that only the L139P mutation, as seen previously (Figure 2A), provided proliferation on medium lacking uracil (Figure

S5A). Upon visualization of mCherry fused to these Fis1p TA mutants, V134P, L139P, A140P, and A144P replacements all clearly diminished mCherry localization to mitochondria (Figure 5B). Our results suggest that the secondary structure of the Fis1p TA is important for its function, and that disruption of helicity at many locations may make targeting to the mitochondrial OM unfavorable.

Curiously, the G137P mutation was not strongly enriched within the mutant pool during selection (Figure 3). Consistent with these results, individual testing of this mutant suggested poor activation of Gal4-dependent transcription (Figure 5A). Moreover, mCherry fused to a Fis1p TA containing the G137P mutation remained strongly localized to mitochondria (Figure 5B). Therefore, proline is not universally unacceptable throughout the MAD of the Fis1p TA.

For those mutant Fis1p TAs that cannot effectively direct mCherry to mitochondria, two mechanisms may explain failure of mitochondrial localization. First, targeting to and insertion at mitochondria may be impeded. Second, these mutant TAs may support initial mitochondrial translocation, but a lack of stability within the lipid bilayer may lead to ejection from the mitochondrial OM by a quality control mechanism. Recently, the yeast Msp1 protein and its human ortholog ATAD1, have been identified as potential 'extractases' that can remove improperly folded or mislocalized proteins from the mitochondrial OM (Okreglak and Walter, 2014; Chen et al., 2014). We tested whether any of tail-anchored fluorescent proteins containing proline replacements and not strongly localized to mitochondria could recover mitochondrial localization in cells deleted of Msp1p. However, deletion of Msp1p did not lead to relocalization of any tested mutant mCherry-TA fusion protein to mitochondria (Figure 5C), providing no evidence for proper targeting, then subsequent removal, of assayed Fis1p TAs harboring proline replacements.

Extension or reduction of Fis1p TA length does not affect targeting to mitochondria

Targeting of tail-anchored proteins to specific membranes may be controlled, at least in part, by the specific length of the MAD domain within the TA (Isenmann et al., 1998; Horie et al., 2002). We reasoned that region within the MAD at which prolines do not strongly disrupt mitochondrial targeting may be amenable to the insertion or deletion of new amino acids, thereby allowing us to test the relationship between Fis1p TA length and mitochondrial targeting. We inserted one (∇1A), two (∇2A), or three (∇3A) additional alanines between A135 and G136 within the TA of Gal4-Fis1p, but none of these mutant constructs led to apparent *HIS3* (Figure 6A) or *URA3* (Figure S5B) activation. We then analyzed the location of mCherry fused to a Fis1p TA carrying these same insertions. All constructs were localized properly to mitochondria (Figure 6B).

Next, we deleted one (ΔG136), two (ΔA135-G136), or three (ΔA135-G137) amino acids within the Fis1p MAD and performed similar assays. Like our insertion mutants, deletion mutants were apparently targeted to a membrane, as assessed by Gal4-driven reporter transcription (Figure 6A and Figure S5B). Moreover, mCherry remained localized to mitochondria when up to three amino acids were deleted (Figure 6C).

Disruption of the ER-localized Spf1 protein reduces the the contrast in ergosterol content between the ER and the mitochondrial OM. Consequently, TAs normally localized to mitochondria are mistargeted to the ER upon Spf1p deletion (Krumpe et al., 2012). The sterol concentration of membranes can determine bilayer thickness (Dufourc, 2008), raising the possibility that insertions or deletions may allow mitochondrial TAs to once again prefer mitochondrial OM targeting over ER localization. However, mCherry linked to insertion and deletion mutants of the Fis1p TA remained prominently localized to the ER in *spf1Δ* mutants (Figure S6).

Together, our results demonstrate that the Fis1p TA allows mitochondrial targeting even when its length is substantially altered.

The hydrophilic carboxyl-terminus of the tail anchor allows specific targeting to mitochondria

Analysis of the data from our deep mutational scan suggested that nonsense mutations throughout much of the TA can allow Gal4-Fis1p to move to the nucleus and activate transcription (Figure 3, Figure 4, and Figure S3). Stop codons placed within the the highly charged RNKRR pentapeptide near the carboxyl-terminus of Fis1p, however, seem to permit some membrane localization. Therefore, we examined the behavior of a R151X mutant, which lacks all charged amino acids following the predicted MAD. Supporting partial localization to a cellular membrane, the R151X mutant of Gal4-Fis1p did not activate Gal4-controlled expression of *HIS3* to the same extent of a Gal4-Fis1p construct lacking the entire TA (Figure 7A), nor did the R151X mutation lead to proliferation on medium lacking uracil (Figure S5C). Consistent with those results, the R151X TA directed mCherry to intracellular organelles (Figure 7B). However, along with some apparent mitochondrial association, the R151X TA was also clearly localized to the ER. Interestingly, ER localization of mCherry fused to the R151X TA occurred independently of Get3p, a receptor for ER tail-anchored proteins (Schuldiner et al., 2008), suggesting an alternative parallel pathway for localization of the R151X TA to the ER (Figure S7). Our results demonstrate that the charged amino acids at the carboxyl-terminus of the TA provide organelle specificity, yet are not totally required for membrane localization. These findings are consistent with previous results reporting that organelle specificity is provided by positively charged amino acids following the MAD (Kuroda et al., 1998; Isenmann et al., 1998; Borgese et al., 2001; Stojanovski et al., 2004).

Since the R151X variant of Gal4-Fis1p activated Gal4-driven reporters, yet was at least partially localized to the ER, we wondered if ER localization of any protein fused to Gal4 might similarly lead to Gal4-driven transcription due to the physical continuity between the ER and nuclear envelope. Therefore, we examined the TA of the human FIS1 protein (hFIS1), since full-length hFIS1 can localize to ER in *S. cerevisiae* (Stojanovski et al., 2004), Indeed, we found that mCherry fused to the hFIS1 TA was mostly localized to ER (Figure S8A). However, a fusion protein consisting of Gal4 fused to the TA of hFIS1 did not provide *HIS3* activation (Figure S8B), indicating that the hFIS1 TA is quantitatively membrane-targeted in *S.*

cerevisiae and that activation of Gal4-dependent reporters upon removal of the positively charged carboxyl-terminus from Gal4-Fis1p is unlikely to be a consequence of ER localization.

Due to the mislocalization of the hFIS1 TA, we then investigated the possibility that other mitochondrial TA proteins from human would be targeted improperly in *S. cerevisiae*. We fused mCherry to the TA of human BAX, a region that is sufficient for insertion at the mammalian mitochondrial OM (Schinzel et al., 2004). While mCherry signal was diminished in comparison with other mCherry fusion proteins examined in this study and expressed under the same promoter, mCherry fused to the BAX TA was properly targeted to mitochondria (Figure S8C). Gal4 fused to the BAX TA did not activate selectable reporters (C. Dunn, unpublished results), suggesting effective mitochondrial targeting mediated by the BAX TA.

Positively charged amino acids are more acceptable than negatively charged amino acids within the predicted transmembrane domain of the Fis1p tail anchor

Our deep mutational scan of the Fis1p TA demonstrated that Gal4-Fis1p was able to activate gene expression when aspartate or glutamate was placed within the MAD (Figure 3). In fact, upon examination of those amino acid replacements in the top three quartiles of counts in the initial library and enriched at least four-fold upon culture in SMM-Trp-His + 20mM 3-AT, 18 of 33 missense mutations converted the native amino acid to aspartate or glutamate (Figure 4). We were surprised to find that placement of positively charged arginine or lysine residues appeared to be much more acceptable within the MAD of Fis1p than aspartate or glutamate; none of the replacements within the high-count, high-enrichment set (Figure 4) were by lysine or arginine.

To further pursue the possibility that positively charged amino acids can be accommodated within the Fis1p MAD, we mutated four amino acids within the hydrophobic stretch of the Fis1p TA to aspartate, glutamate, lysine, or arginine. Specifically, we generated amino acid replacements at V132, A140, A144, or F148. We subsequently retested these mutants under selection for Gal4-Fis1p transcriptional activity. The results from our global analysis were verified, with aspartate and glutamate mutations providing stronger reporter activation than lysine and arginine mutations (Figure 8), except for the V132D mutant, which did not provide histidine prototrophy. Only the A144D mutation provided sufficient Gal4 activation for proliferation on medium lacking uracil (Figure S5D), suggesting a very severe TA localization defect caused by this TA mutation. We noted that these mutant Gal4-Fis1 constructs exhibit altered behavior at low temperature; positively charged amino acids clearly led to increased *HIS3* activity at 18˚C at positions A140 and F148 (Figure S9). This outcome is consistent with the idea that altered phospholipid dynamics at reduced temperature may lead to consequent changes to TA insertion efficiency (de Mendoza and Cronan, 1983).

We then tested the ability of these charged Fis1p TAs to promote mitochondrial localization of mCherry. At V132 and F148, positions within the MAD nearer to the putative water-lipid bilayer interface, mutation to positively charged amino acids

allowed near wild-type localization to mitochondria (Figure 9A). In contrast, mutation to negatively charged amino acids hindered mitochondrial targeting. We noted that F148D and F148E replacements hindered mitochondrial localization more severely than V132D and V132E replacements. At position A144, lying more deeply within the MAD, all charge mutations inhibited mCherry targeting to mitochondria to some degree, but TAs containing A144D and A144E were less able to localize to mitochondria than A144K or A144R. Finally, no mitochondrial localization was apparent for any of the charge mutants tested at position A140. However, A140K and A140R mutants differed from A140D and A140E mCherry-TA mutants by localizing to other membranes within the cell, including the plasma membrane, rather than providing a diffuse cytosolic signal. Taken together, our results demonstrate that positively charged amino acids at several mitochondrial TA positions do not prohibit mitochondrial targeting and are clearly more acceptable than negatively charged amino acids at those same positions.

We then tested whether deletion of the OM extractase Msp1p might allow those charged Fis1p TAs that poorly localize to mitochondria to recover their targeting to this organelle. However, Msp1p removal did not permit relocalization of tail-anchored fluorescent proteins to mitochondria (Figure 9B). These data support the idea that charge replacements within the Fis1p TA lead to a failure of association with the OM rather than enhanced removal from mitochondria.

We carried out assays to determine if Fis1p carrying charge mutations within their TAs at V132, A144, or V148 can provide Fis1p activity. Negligible Fis1p activity at mitochondria is apparently sufficient to promote mitochondrial fission (Habib et al., 2003; Krumpe et al., 2012), suggesting that even minimal localization and related functionality at the OM would be detectable by functional assays. For example, when Fis1p activity is absent, mitochondrial fission cannot proceed and unchecked fusion leads to a unified mitochondrial network (Mozdy et al., 2000). Interestingly, Fis1p variants harboring charged residues, positive or negative, at positions V132, A144, or V148 provided some Fis1p function when expressed from a plasmid in a *fis1Δ* background, with the exception of the Fis1p carrying the A144D mutation, as indicated by mitochondrial morphology (Figure 10A). To further investigate Fis1p activity, mitochondrial morphology was further perturbed by treatment with sodium azide, which leads to mitochondrial fragmentation in cells competent for mitochondrial division (Klecker et al., 2015; Fekkes et al., 2000) and to facile visualization of mitochondrial fission defects. Again, except for the A144D mutant, all Fis1p variants tested were able to provide mitochondrial division activity (Figure 10B and Figure S10).

Next, we applied a genetic test of Fis1p function. When mitochondrial fusion is blocked, unbalanced mitochondrial division leads to mitochondrial fragmentation (Rapaport et al., 1998; Hermann et al., 1998), and mtDNA and the ability to respire are rapidly lost. If mitochondrial division is lacking, however, mtDNA is maintained by cells unable to carry out mitochondrial fusion (Sesaki and Jensen, 1999; Tieu and Nunnari, 2000; Mozdy et al., 2000; Fekkes et al., 2000). In a result consistent with our microscopy-based analysis, we found that only the A144D variant of Fis1p lacked activity and therefore allowed cells to maintain mtDNA when mitochondrial

fusogen Fzo1p is removed (Figure 10C). All other variants provided sufficient fission activity for mitochondrial fragmentation and mtDNA loss in the absence of Fzo1p. We note that upon selection for Gal4-driven reporter activation, only the A144D charge mutant provided sufficient *URA3* activation for proliferation on medium lacking uracil (Figure S5D), supporting the correspondence between each mutant TA's targeting, as reported by Gal4-Fis1p transcriptional activity, and is functionality at the mitochondrial surface. Taken together, our results demonstrate that positively charged amino acids within the MAD can better promote Fis1p localization than negatively charged amino acids, but that even negatively charged amino acids can be accommodated within the MAD and lead to some low level of mitochondrial targeting.

DISCUSSION:

Using a deep mutational scanning approach, we examined structural characteristics of the Fis1p TA important for targeting to the mitochondrial outer membrane. To our knowledge, this work is the first application of this systematic approach to the study of a eukaryotic organelle targeting signal. Deep mutational scanning, when coupled to an effective method of screening or selection, is very cost- and time-effective (Boucher et al., 2014; Fowler and Fields, 2014; Araya and Fowler, 2011). Mutant library generation, subsequent pool selection, and next-generation sequencing were completed in just a few months. Consequently, this approach generates far more useful data over a shorter duration than, for example, alanine scanning mutagenesis or low-throughput genetic selection followed by Sanger sequencing. Deep mutational scanning has recently been applied successfully to other areas of study, such as membrane protein insertion within bacteria (Elazar et al., 2016), tumor suppressor structure and function (Starita et al., 2015), and the relationship between a polypeptide's evolutionary path and its present fitness (Hietpas et al., 2011; Melamed et al., 2013)

Positively charged amino acids within mitochondrial tail anchors may "snorkel" to the lipid bilayer surface

Because there is a high energetic barrier to placing any charged residue into a lipid bilayer (Cymer et al., 2015), we were initially surprised to find that positively charged amino acids within the MAD of the Fis1p TA promoted mitochondrial targeting far better than negatively charged amino acids. However, it has been suggested that lysine and arginine within a MAD can "snorkel," or integrate the uncharged portion of their side chain into the hydrophobic milieu of the lipid bilayer and locate their positive charges near polar head groups at the interface between the membrane and aqueous environment (Monné et al., 1998; Strandberg and Killian, 2003; Segrest et al., 1990; Schow et al., 2010). The shorter hydrophobic portion of aspartate and glutamate may not permit the side chain to easily reach the membrane interface in order to remove the negative charge from the hydrophobic environment, thereby making such mutants less prone to stable insertion at the lipid bilayer. Snorkeling has been visualized, for instance, during structural studies of the Kv1.2 potassium channel (Long et al., 2005) and integrin β3 (Kim et al., 2012). However, little *in vivo* functional evidence has been reported supporting the snorkeling of amino acids located within MADs. Our deep mutational scan of the Fis1p TA, a region for which the sole purpose is to direct mitochondrial OM integration (Kemper et al., 2008; Habib et al., 2003), strongly suggests the ability of lysine or arginine to be accommodated by snorkeling at numerous positions within the Fis1p MAD. We note that snorkeling, if operative for positive charges within the Fis1p TA, may not be permitted within the context of all mitochondrial TAs: replacement of S184 within the BAX TA by lysine does not seem to permit mitochondrial localization of this protein (Nechushtan et al., 1999).

The membrane-associated domain of the Fis1p tail-anchor may consist of two separable segments

Computational analyses suggest that the Fis1p TA is mostly alpha-helical in nature (Drozdetskiy et al., 2015; Buchan et al., 2013). We found that proper localization of the Fis1p TA likely requires its predicted alpha-helicity within the MAD, since proline, which is known to break or kink helices (Senes et al., 2004), profoundly disrupts targeting at many positions throughout this hydrophobic region. However, we found that replacement by proline is more acceptable at a specific location, G137, than proline mutations found at previous or subsequent locations within the MAD, potentially indicating that the Fis1p MAD is bipartite in nature. Further supporting a bipartite structure of the Fis1p MAD, insertion of new amino acids between A135 and G136 did not apparently affect mitochondrial TA targeting. Moreover, mutations toward the carboxyl-terminal end of the Fis1p MAD appear to affect mitochondrial targeting more drastically, as reported by deep mutational scanning, than mutations toward the amino terminus of the transmembrane segment. Previous analysis of the yeast Tom5p TA and rat OMP25 TA also support a bipartite structure of the MAD, with higher sensitivity to mutation nearer to the carboxyl-terminal end of this hydrophobic stretch (Horie et al., 2002). Indeed prolines are found within the MAD of the mammalian OMb and OMP25 TAs, and a proline within the MAD of Tom5p, whose TA appears similar to that of Fis1p with respect to its helical MAD and positively charged carboxyl-terminus, is important for targeting to mitochondria (Allen et al., 2002). These results suggest that those prolines might demarcate the boundary between distinct structural regions of the targeting sequence. On the other hand, prolines within a single helical segment may simply be more easily housed within an alpha-helix when buried deep in the lipid bilayer (Senes et al., 2004; Li et al., 1996) and may not reflect two separable MAD segments. If this is the case, prolines found in mitochondria TAs might indicate the portion of the TA found at the midpoint of the OM.

Glycine is not preferred within alpha-helices (Chou and Fasman, 1974; O'Neil and DeGrado, 1990) as a consequence of its conformational flexibility. However, our deep mutational scan does not indicate reduced membrane targeting when most amino acids within the Fis1p TA are individually mutated to glycine. This might be surprising in light of the pronounced effects provided by several proline replacement mutations throughout this domain. However, glycine may not be as disruptive for alpha-helices found within a lipid bilayer environment when compared with alpha-helices of soluble proteins, due to better intra-helical hydrogen bonding within the hydrophobic environment of the membrane (Dong et al., 2012). Indeed, four glycines already exist within the *S. cerevisiae* Fis1p TA. The TAs of Fis1p orthologs are also littered with glycines (Stojanovski et al., 2004), further indicating that glycines are less disruptive of the Fis1p TA than prolines. Interestingly, GXXXG motifs, and other similarly spaced small amino acids like alanine and serine, can promote helix packing within lipid bilayers (Senes et al., 2004; Russ and Engelman, 2000; Gimpelev et al., 2004). However, our findings demonstrate that the sole Fis1p GXXXG motif and a nearby AXXXA motif do not play a significant role in targeting of the Fis1p TA to the OM.

The Fis1p tail anchor may not be exposed to the intermembrane space

Four of five carboxyl-terminal residues of Fis1p are positively charged. Previous reports indicated that a positively charged carboxyl-terminus is important specifically for proper Fis1p targeting and generally for insertion of several other TAs at the mitochondrial OM (Isenmann et al., 1998; Horie et al., 2002; 2003; Stojanovski et al., 2004; Habib et al., 2003; Yoon et al., 2003). Further supporting the importance of this highly charged region, our genetic selection and subsequent microscopic analysis revealed that the last five amino acids within the Fis1p sequence are important for effective mitochondrial OM targeting. How this charged region promotes mitochondrial localization is not yet clear.

The currently accepted view of Fis1p topology is that this positively charged carboxyl-terminus is ultimately exposed to the mitochondrial intermembrane space. However, a presumably high energetic barrier (Engelman and Steitz, 1981; Honig and Hubbell, 1984; Parsegian, 1969) makes it difficult to countenance the transfer of the highly charged carboxyl-terminus of mitochondrial TA proteins across a lipid bilayer without the assistance of an aqueous pore. Interestingly, organellar import of mitochondrial TA-containing proteins appears saturable in mammalian cells (Setoguchi et al., 2006), potentially indicating a finite number of translocons capable of transporting mitochondrial TAs. Furthermore, the TOM complex has been reported to assist in insertion of full-length BAX into mitochondria (Ott et al., 2007; Colin et al., 2009; Cartron et al., 2008). Potentially consistent with the need for a mitochondrial TA translocation machinery, the hFIS1 TA localizes specifically to mitochondria in human cells (Suzuki et al., 2003), but cannot effectively localize mCherry to *S. cerevisiae* mitochondria, possibly suggesting evolutionary divergence and a structural mismatch between the hFIS1 TA and the putative yeast TA translocation apparatus. However, we note that not all human mitochondrial TAs fail to be imported at the proper organelle in yeast, since our genetic and microscopic results indicate that human BAX TA is properly inserted into yeast mitochondria.

On the other hand, stronger evidence supports the idea that mitochondrial tail-anchored proteins like Fis1p can spontaneously insert into the OM. First, the MAD of the TA is protected from chemical modification upon exposure to lipid vesicles devoid of protein (Kemper et al., 2008), suggesting that the Fis1p TA can spontaneously insert into lipid bilayers. Moreover, blockade or destruction of the general insertion pore for mitochondrial proteins and its associated receptors does not prevent Fis1p insertion into yeast mitochondria, and tail-anchored proteins appear to spontaneously and rapidly insert into mammalian mitochondria without the need for the TOM complex or soluble cytosolic chaperones (Setoguchi et al., 2006). Further supporting the absence of a translocation machinery for these TAs, a large-scale screen for proteins required for proper localization of mitochondrial tail-anchored proteins uncovered no putative translocon components (Krumpe et al., 2012). Finally, although not evaluated in this work due to strong repression of peroxisome biogenesis under the culture conditions utilized (Einerhand et al., 1991; Van der Leij et al., 1993), a small fraction of cellular Fis1p may function at peroxisomes to mediate peroxisomal fission (Kuravi et al., 2006; Koch et al., 2005).

A machinery that allows Fis1p TA insertion would potentially be shared by both mitochondria and peroxisomes, but no dual-localized translocation machinery has yet been identified.

How can one reconcile abundant evidence for spontaneous insertion of TAs into the mitochondrial OM with the presence of a highly charged region at the carboxyl-terminus of the Fis1p TA that has been assumed to be translocated? We suggest the possibility that while the Fis1p TA is likely to be inserted into the mitochondrial OM, it does not pass all the way through to the intermembrane space. Rather, the TA may be buried within the outer leaflet of the OM, making transit of the positively charged terminus through the lipid bilayer unnecessary. Such a scenario is supported by studies indicating that the TA-containing protein BAX is constantly targeted to the mitochondrial OM in non-apoptotic cells, then removed from the mitochondrial surface and returned to the cytosol (Edlich et al., 2011; Schellenberg et al., 2013). Constitutive extraction of BAX that has completely passed through the OM and exposes polypeptide to the intermembrane space seems unnecessarily expensive from an energetic standpoint. Rather, it is conceivable that the TA of inactive BAX is monotopically integrated within the plane of the membrane, thereby facilitating recycling. If true, Fis1p may take on a similar topology due to structural similarity between the BAX and Fis1p TAs. Moreover, the snorkeling of lysine or arginine placed into the Fis1p TA that is suggested by findings reported here is consistent with both bitopic and monotopic insertion (Strandberg and Killian, 2003). Finally, contrary to studies of other mitochondrial TA proteins (Isenmann et al., 1998; Horie et al., 2002), our work suggests that a specific MAD length is not crucial for Fis1p mitochondrial targeting. If the Fis1p TA passes completely through the OM, deletion of three amino acids from the MAD might lead to unfavorable placement of flanking charges into the hydrophobic domain, and consequently, at least some reduction in mitochondrial insertion. In contrast, sidelong placement of the TA in the outer leaflet of the OM might easily tolerate shortening of the TA without an energetic penalty, as is indicated by normal localization of deletion mutants. A caveat regarding any model in which Fis1p is monotopic at the OM is that neither the WT Fis1p TA nor any functional TA charge mutants produced in this study are characterized by the predicted amphiphilicity that is thought to promote oblique insertion at membranes (Sapay et al., 2006).

Computational modeling informed by our high-throughput dataset, as well as further experimental work, will allow testing of whether Fis1p is monotopic or truly passes through the mitochondrial OM. Moreover, if a TA insertion machinery does exist at the mitochondrial OM, loss-of-function mutations affecting this machinery would presumably be recovered by the application of our genetic selection scheme. Finally, refined analysis of other organelle targeting signals and membrane insertion sequences can be accomplished by applying the deep mutational scanning approach outlined in this study.

METHODS:

Yeast strains and plasmids

Details of strains used in this study are provided in Table S2. Plasmid acquisition details and associated references, as well as details of plasmid construction, are found in Table S3. Oligonucleotides used in this study are listed in Table S4.

Culture conditions

Synthetic complete (SC) medium contains 0.67% yeast nitrogen base without amino acids, 2% dextrose, 0.1% casamino acids, 50 µg/ml adenine hemisulfate, and either 25 µg/ml uracil (SC-Trp) or 100 µg/ml L-tryptophan (SC-Ura). Supplemented minimal medium (SMM) medium contains 0.67% yeast nitrogen base without amino acids, 2% dextrose, 20 µg/ml adenine hemisulfate, 20 µg/ml uracil, 20µg/ml methionine, 30 µg/ml lysine. SMM also contains, depending on selection needs, 20 µg/ml histidine, 100 µg/ml leucine, and/or 20 µg/ml tryptophan, as indicated. SLac medium lacking histidine contains 0.67% yeast nitrogen base without amino acids, 1.2% NaOH, a volume of lactic acid sufficient to subsequently bring the pH to 5.5, 20 µg/ml adenine hemisulfate, 20 µg/ml uracil, 20 µg/ml methionine, 30 µg/ml lysine, 100 µg/ml leucine, and 20 µg/ml tryptophan. Solid media also contain 1.7% bacteriological agar. Cells were incubated at 30˚C unless indicated. For serial dilution assays, strains in logarithmic proliferation phase were diluted to an OD_{600} of 0.1, and 4 µL of this dilution and three serial five-fold dilutions were spotted to solid medium.

Microscopy

For epifluorescence microscopy, cells in the logarithmic phase of proliferation were examined using an Eclipse 80i microscope with a 100X Plan Fluor objective and linked to a DS-Qi1Mc camera (Nikon, Tokyo, Japan). Cells were cultured in SMM medium appropriate for plasmid selection. Exposure times were automatically determined, and images were captured using NIS-Elements version AR 3.2. All images of mCherry expression were equivalently brightness adjusted in Adobe Photoshop CS5 (Adobe, San Jose, California), except when the mCherry-BAX(TA) signal was assessed. In this case, the 'autolevels' adjustment was used. Scoring of mitochondrial morphology was performed blind to genotype. To promote mitochondrial fragmentation, sodium azide was added at a concentration of 500 µM for 60 min before fluorescence microscopy.

Fis1p TA mutant library construction

Recombination-based cloning (Oldenburg et al., 1997) was used generate constructs expressing Gal4-Fis1p and mutated at one of 27 positions within the Fis1p TA. Two DNA segments generated by PCR were fused in this recombination reaction. The 5' portion was amplified by PCR from template plasmid b100 using primer 698 and the appropriate primer (rvsposX) listed in Table S4. The 3' section was generated from template b100 using primers 517 and the relevant primer

(fwdposX) listed in Table S3. PCR products were recombined into *Not*I-linearized pKS1 by co-transformation of vector and PCR products into strain MaV203. Each sub-library for each Fis1p TA position was generated individually by selection of Trp^+ clones in liquid medium, with a portion of each transformation reaction plated to solid SC-Trp medium to confirm recombination and transformation efficiency. To generate the total pool prior to selection for Gal4p-mediated transcription, equal numbers of cells, as determined by OD_{600} measurement, were taken from overnight cultures of each sub-library and combined within the same liquid culture. Note that all constructs expressing Gal4-Fis1p also contain superfolder GFP in frame between the Gal4p and Fis1p segments, but for simplicity, this is omitted from figure labels and from the text.

Deep mutational scanning of the Fis1p TA library

The pool of constructs containing Fis1p TA mutations was cultured for four generations in SC-Trp medium, SC-Ura medium, or SMM-Trp-His medium containing 0 mM, 5 mM, 10 mM, or 20 mM 3-AT. Plasmids present under each culture condition were then harvested from 10 OD_{600} units of cells. To harvest each plasmid library, cells were pelleted at 4,000g for 3 min, then washed with 5 ml 0.9 M D-sorbitol and resuspended in 1 ml of 0.9 M D-sorbitol. One "stick-full" of zymolyase 20T (Amsbio, Abingdon, United Kingdom), was added, and cells were incubated at 37˚C for 45 min. Cells were again collected at 4,000g for 3 min and processed using a plasmid purification kit (GeneJET Plasmid Miniprep Kit, Thermo Scientific, Waltham, USA) using the manufacturer's instructions. Primers 882 and 883 were used to amplify the genomic region encoding the Fis1p TA from each plasmid pool. Using the provided PCR products, next-generation, paired-end sequencing was performed by Microsynth (Balgach, Switzerland) on a MiSeq Nano (2x150v2). The resulting FASTQ output can be found at [to be uploaded to repository]. FASTQ output from paired ends and lacking adaptor sequences was combined into a single segment using the PANDAseq assembler version 2.8 (Masella et al., 2012). The TRIM function (trimmer Galaxy tool version 0.0.1) was performed using the resources of the Galaxy Project (Goecks et al., 2010) in order to remove sequences not directly encoding the defined Fis1p and stop codon. Further processing in Microsoft Excel (Redmond, USA) subsequently allowed conversion of DNA sequence to amino acid sequence and removal of those TAs with more than one amino acid mutation from further analysis. Enrichment values reflect, at a given amino acid position, the ratio of the fraction of amino acid counts following selection to the fraction of amino acid counts in the starting library. Enrichment values are not derived through comparisons across different amino acid positions. Counts for the native amino acid at each position were set as the total number of TA counts for which all amino acids were wild-type within a given selected pool. When calculating enrichment values, TA amino acid replacements for which there were zero reads in the SC-Trp sample had their value changed to one in order to allow possible detection of enrichment under selective conditions by preventing division by zero. Heat maps were generated using the Matrix2png utility (Pavlidis and Noble, 2003).

ACKNOWLEDGEMENTS:

We thank Gülayşe İnce Dunn, Bengisu Seferoğlu, Güleycan Lutfullahoğlu, Funda Kar, and Sara Nafisi for comments on this manuscript. This work was supported by a European Research Council Starting Grant (637649-RevMito) to CDD, by a European Molecular Biology Organization Installation Grant (2138) to CDD, and by Koç University.

CONFLICT OF INTEREST STATEMENT:

The authors have no known conflict of interest affecting the outcome or interpretation of this study.

FIGURE LEGENDS:

Figure 1. A genetic selection based on protein mislocalization allows recovery of mutations blocking Fis1p TA localization to mitochondria. (A) A scheme for selection of mutations preventing mitochondrial targeting of the Fis1p TA. Full-length Fis1p is fused to the transcription factor Gal4p (and to superfolder GFP, not shown). Upon failure to localize Fis1p at the mitochondrial OM, Gal4p is free to translocate to the nucleus and activate *HIS3* and *URA3*. (B) Removal of the Fis1p TA allows proliferation on medium requiring *HIS3* activation or *URA3* activation. Strain MaV203 expressing Gal4-Fis1p variants from plasmids b100 (WT), b101 (ΔTA), or harboring empty vector pKS1 was cultured in SC-Trp medium, then, following serial dilution, spotted to SC-Trp, SMM-His + 20 mM 3-AT, or SC-Ura for 2 d.

Figure 2. Selection for reporter activation by Gal4-Fis1p reveals TA mutations required for full mitochondrial localization. (A) Missense mutations within the Fis1p TA provide selectable marker activation. Strain MaV203 expressing Gal4-Fis1p variants from plasmids b100 (WT), b128 (V145E), b129 (L139P), b130 (L129P, V138A), or b101 (ΔTA) were treated as in Figure 1B. (B) Missense mutations within the Fis1p TA allow cytosolic accumulation of a linked mCherry protein. mCherry fused to variants of the Fis1p TA were expressed in WT strain CDD961 from plasmids b109 (WT), b134 (V145E), b135 (L139P), b136 (L129P,V138A), or b252 (ΔTA) and visualized by fluorescence microscopy. Mitochondria were labelled with a mitochondria-targeted GFP expressed from plasmid pHS1. Scale bar, 5 μm.

Figure 3. Mutations within the TA of a Gal4-Fis1 fusion protein allow Gal4-driven transcription. Log_2 of enrichment values for each amino acid were calculated for each position following selection in SMM-Trp-His medium containing 20 mM 3-AT. Enrichment values are generated for individual amino acid positions within the TA, and not across positions. Black outlines denote the native amino acid for each position. Amino acid replacements not detectable under selective conditions are denoted by black, filled squares. The predicted MAD is indicated by a red line.

Figure 4. Identification of abundant Gal4-Fis1p clones which are highly enriched upon selection for Gal4-Fis1p nuclear translocation. (A) TA replacement mutations are plotted, with log_2 enrichment values provided on the X-axis, and sequence counts recovered from the starting pool (SC-Trp) provided on the Y-axis. Those replacement mutations that are within the top 75th percentile of mutant abundance in the starting pool and enriched at least four-fold following selection in SMM-Trp-His medium containing 20 mM 3-AT are highlighted in a blue box. (B) Expansion of the highlighted region in (A) showing specific TA mutations.

Figure 5. Proline is not favored at several locations within the Fis1p TA. (A) Replacement of amino acids within the TA of Gal4-Fis1p with proline can lead to Gal4-mediated selectable marker activation. Strain MaV203 expressing Gal4-Fis1p variants from plasmids b100 (WT), b188 (V134P), b189 (G137P), b135 (L139P), b190 (A140P), b191 (A144P), or b101 (ΔTA) was cultured in SC-Trp medium then spotted to SC-Trp or SMM-His + 20 mM 3-AT medium for 2 d. (B) TAs with proline replacements can reduce mitochondrial targeting of a linked fluorescent protein.

mCherry fused to variants of the Fis1p TA were expressed in wild-type strain CD961 from plasmids b109 (WT), b208 (V134P), b209 (G137P), b135 (L139P), b210 (A140P), b211 (A144P) and examined, along with mitochondria-targeted GFP, as in Figure 2B. (C) Deletion of the Msp1p extractase does not allow tail-anchored proteins mistargeted due to proline inclusion to return to mitochondria. Cells from *msp1Δ/msp1Δ* strain CDD1044 expressing pHS1 and plasmids b109 (WT), b208 (V134P), b135 (L139P), b210 (A140P), or b211 (A144P) were inspected as in Figure 2B. Scale bar, 5 μm.

Figure 6. Targeting of the Fis1p TA is not dependent upon a specific TA length. (A) Deletion of up to three amino acids or insertion of up to three amino acids does not allow Gal4-Fis1p to activate transcription. Mav203 cells expressing Gal4-Fis1p variants from plasmids b229 (∇1A), b230 (∇2A), b231 (∇3A), b226 (ΔG136), b227 (ΔA135-G136), b228 (ΔA135-G137), or b101 (ΔTA) were treated as in Figure 5A. (B) mCherry fused to a Fis1p TA containing an insertion of up to three amino acids in length localizes properly to mitochondria. Strain CDD961 expressing mCherry-TA fusions from plasmids b109 (WT), b235 (∇1A), b236 (∇2A), or b237 (∇3A) was visualized as in Figure 2B. (C) mCherry fused to a Fis1p TA deleted of up to three amino acids is properly targeted to mitochondria. Strain CDD961 expressing mCherry-TA fusions from plasmids b109 (WT), b232 (ΔG136), b233 (ΔA135-G136), or b234 (ΔA135-G137) was examined as in Figure 2B. Scale bar, 5 μm.

Figure 7. The positively charged carboxyl-terminus of the Fis1p TA is important for specific localization to at the mitochondrial outer membrane. (A) Deletion of the final five amino acids from the Fis1p TA permits transcriptional activation by Gal4-Fis1p. Strain Mav203 harboring plasmids b100 (WT), b253 (R151X), or b101 (ΔTA) were treated as in Figure 5A. (B) Removal of the last five amino acids from the Fis1p TA allows mislocalization to the ER. Strain CDD961 expressing mCherry fused to the WT Fis1p TA (b109) or expressing mCherry linked to a truncated Fis1p TA (R151X) from plasmid b254 were evaluated as in Figure 2B. Scale bar, 5 μm.

Figure 8. Negative charges allow higher transcriptional activity than positive charges when placed at specific positions within the Gal4-Fis1p TA. Strain MaV203 was transformed with plasmids pKS1 (vector), b100 (Gal4-Fis1), b101 (Gal4-Fis1(ΔTA)), or plasmids encoding the indicated charge replacements within the Fis1p TA (plasmids b172- b187). The resulting transformants were treated as in Figure 5A.

Figure 9. Positive charges are more acceptable during targeting of the Fis1p TA to mitochondria than negative charges. (A) Examination of mCherry-TA localization in WT cells expressing Msp1p. Strain CDD961 was transformed with plasmids expressing mCherry linked to the Fis1p TA harboring the indicated charge replacements from plasmids b192-b207. Cells were visualized as in Figure 2B. (B) Deletion of Msp1p does not allow recovery of mitochondrial localization by poorly targeted mCherry-TA variants. Strain CDD1044, deleted of Msp1p, was transformed with the following plasmids encoding mCherry fused to the mutant TAs: b192 (V132D), b196 (A140D), b197 (A140E), b198 (A140K), b199 (A140R), b200 (A144D),

b201 (A144E), b134 (V145E), b204 (F148D), b205 (F148E). Transformants were examined as in Figure 2B. Scale bar, 5 μm.

Figure 10. Positive and negative charge replacements within the TA can generally support Fis1p function. (A) Normal mitochondrial morphology can be maintained even when charges are placed within the hydrophobic MAD of the Fis1p TA. Strain CDD741 was transformed with pRS313, a plasmid expressing WT *FIS1* (b239), or a plasmid expressing *FIS1* harboring a mutation that leads to the indicated TA alteration (plasmids b240-251). Mitochondrial morphology was visualized by expression of mitochondria-targeted GFP from plasmid pHS12. Scale bar, 5 μm. (B) Induced, Fis1p-dependent mitochondrial fragmentation is permitted by charge placement within the Fis1p TA. Transformants analyzed in (A) were treated with sodium azide to provoke mitochondrial fragmentation, and cells were scored for the maintenance of a mitochondrial network (n=200 cells). (C) Charged residues within the TA provide exhibit Fis1p activity during a genetic assay of Fis1p function. *fzo1Δ fis1Δ* strain CDD688, carrying a CHX-counterselectable, *FZO1*-expressing plasmid, was transformed with the *FIS1*-expressing plasmids enumerated above. Transformants were cultured overnight in SMM-His medium to permit cells to lose the *FZO1*-encoding plasmid. Serial dilutions were spotted to SLac-His+3 μg/mL CHX and incubated for 5 d to test for maintenance of mtDNA following counterselection for *FZO1*. As a control for cell proliferation under conditions not strongly selective for mtDNA maintenance, cells were also spotted to SMM-Trp-His medium and incubated for 2 d.

Figure S1. Fusion to the Fis1p TA constrains Pdr1p activity. Strain BY4743 was transformed with plasmid b158 (Pdr1-Fis1(TA) WT), b159 (Pdr1-Fis1(TA) V145E), b160 (Pdr1-249-Fis1(TA) WT), b165 (Pdr1-249-Fis1(TA) V145E), or empty vector pRS316. Cells were cultured in SC-Ura medium, then spotted to SC-Ura medium or SC-Ura medium containing 0.2 μg/ml CHX and incubated for 2 d.

Figure S2. An examination of amino acid replacement representation within the Fis1p TA library. The fraction of counts representing each amino acid replacement in the starting SC-Trp library (fObs) was compared to the fraction that would be expected based on randomized codon recovery (fExp). Native amino acids are represented by a black square with a blue dot. Amino acid replacements with no representation in the library are represented by empty black squares. The predicted MAD is indicated by a red line.

Figure S3. Amino acid replacement frequencies within the Fis1p TA suggest that assessing histidine auxotrophy in the presence of 3-AT may provide the most informative results regarding Gal4-Fis1p location. Quantification of replacement in SMM-Trp-His medium without 3-AT (A), containing 5 mM 3-AT (B), containing 10mM 3-AT (C), or in SC-Ura medium (D). In all panels, black outlines indicate the native amino acid at each position within the Fis1p TA. Amino acid replacements not detectable under selective conditions are denoted by black, filled squares. The predicted MAD is indicated by a red line.

Figure S4. Little evidence for codon-level control of Gal4-Fis1p TA targeting. Log_2 of enrichment values for each codon following selection of the Fis1p TA library in SMM-Trp-His medium containing 20 mM 3-AT are illustrated. Green outlines denote the native amino acid at each position. Codon replacements with no representation in the library following selection are represented by empty black squares. The predicted MAD is indicated by a red line.

Figure S5. Uracil auxotrophy tests that were performed alongside histidine auxotrophy tests. Samples cultured in SC-Trp for (A) Figure 5A, (B) Figure 6A, (C) Figure 7A, and (D) Figure 8 were also spotted to SC-Ura medium and incubated for 2 d.

Figure S6. mCherry fused to Fis1p TAs of varying length remains targeted to the ER in *spf1Δ* mutant cells. (A) Strain CDD1031, lacking Spf1p and expressing mCherry-TA fusions from plasmids b109 (WT), b235 (∇1A), b236 (∇2A), or b237 (∇3A), b232 (ΔG136), b233 (ΔA135-G136), or b234 (ΔA135-G137) were examined as in Figure 2B.

Figure S7. A mutated Fis1p TA lacking the positively charged carboxyl-terminus localizes to the ER independent of Get3p expression. *get3Δ/get3Δ* strain CDD1033 expressing mCherry fused to a WT Fis1p TA from plasmid b109 or expressing mCherry fused to a Fis1p TA lacking the positively charged carboxyl-terminus (R151X) from plasmid b254 were examined as in Figure 2B. Mitochondria were labelled with GFP expressed from pHS1.

Figure S8. The TAs of human proteins do not universally target to mitochondria in yeast. (A) The hFIS1 TA is mistargeted to the ER in *S. cerevisiae*. Strain CDD961 containing plasmid b257 expressing mCherry fused to the hFIS1 TA was analyzed as in Figure 2B. (B) The hFIS1 TA does not permit activity of a fused Gal4p within the nucleus. Strain MaV203 was transformed with plasmid b100 (Gal4-Fis1), b258 (Gal4-hFIS1(TA)), or plasmid b101 (Gal4-Fis1ΔTA) and assessed as in Figure 5A. (C) The BAX TA can target to mitochondria in *S. cerevisiae*. Strain CDD961 transformed with plasmid b255, which expresses mCherry fused to the BAX TA, was examined as in Figure 2B.

Figure S9. Temperature affects the outcome of adding a positive charge to the Fis1p TA. Samples used in Figure 8 were also spotted to SMM-His medium containing 20 mM 3-AT and incubated at 37˚C for 3 d (A) or 18˚C for 5 d (B).

Figure S10. Most charge replacements within the Fis1p MAD permit Fis1p-dependent mitochondrial fragmentation. Images of azide-treated cells examined in Figure 10B are provided.

REFERENCES:

Allen, R., B. Egan, K. Gabriel, T. Beilharz, and T. Lithgow. 2002. A conserved proline residue is present in the transmembrane-spanning domain of Tom7 and other tail-anchored protein subunits of the TOM translocase. *FEBS Lett*. 514:347–350.

Araya, C.L., and D.M. Fowler. 2011. Deep mutational scanning: assessingprotein function on a massive scale. *Trends in Biotechnology*. 29:435–442. doi:10.1016/j.tibtech.2011.04.003.

Borgese, N., I. Gazzoni, M. Barberi, S. Colombo, and E. Pedrazzini. 2001. Targeting of a tail-anchored protein to endoplasmic reticulum and mitochondrial outer membrane by independent but competing pathways. *Mol Biol Cell*. 12:2482–2496.

Borgese, N., S. Brambillasca, and S. Colombo. 2007. How tails guide tail-anchored proteins to their destinations. *Current opinion in cell biology*. 19:368–375. doi:10.1016/j.ceb.2007.04.019.

Boucher, J.I., P. Cote, J. Flynn, L. Jiang, A. Laban, P. Mishra, B.P. Roscoe, and D.N.A. Bolon. 2014. Viewing protein fitness landscapes through a next-gen lens. *Genetics*. 198:461–471. doi:10.1534/genetics.114.168351.

Buchan, D.W.A., F. Minneci, T.C.O. Nugent, K. Bryson, and D.T. Jones. 2013. Scalable web services for the PSIPRED Protein Analysis Workbench. *Nucleic Acids Res*. 41:W349–57. doi:10.1093/nar/gkt381.

Cartron, P.-F., G. Bellot, L. Oliver, X. Grandier-Vazeille, S. Manon, and F.M. Vallette. 2008. Bax inserts into the mitochondrial outer membrane by different mechanisms. *FEBS Lett*. 582:3045–3051. doi:10.1016/j.febslet.2008.07.047.

Chen, Y.-C., G.K.E. Umanah, N. Dephoure, S.A. Andrabi, S.P. Gygi, T.M. Dawson, V.L. Dawson, and J. Rutter. 2014. Msp1/ATAD1 maintains mitochondrial function by facilitating the degradation of mislocalized tail-anchored proteins. *EMBO J*. 33:1548–1564. doi:10.15252/embj.201487943.

Chou, P.Y., and G.D. Fasman. 1974. Conformational parameters for amino acids in helical, beta-sheet, and random coil regions calculated from proteins. *Biochemistry*. 13:211–222.

Colin, J., J. Garibal, B. Mignotte, and I. Guenal. 2009. The mitochondrial TOM complex modulates bax-induced apoptosis in Drosophila. *Biochemical and Biophysical Research Communications*. 379:939–943. doi:10.1016/j.bbrc.2008.12.176.

Cymer, F., G. von Heijne, and S.H. White. 2015. Mechanisms of Integral Membrane Protein Insertion and Folding. *J Mol Biol*. 427:999–1022. doi:10.1016/j.jmb.2014.09.014.

de Mendoza, D., and J.E. Cronan Jr. 1983. Thermal regulation of membrane lipid

fluidity in bacteria. *Trends in Biochemical Sciences*. 8:49–52. doi:10.1016/0968-0004(83)90388-2.

Denic, V., V. Dötsch, and I. Sinning. 2013. Endoplasmic reticulum targeting and insertion of tail-anchored membrane proteins by the GET pathway. *Cold Spring Harbor Perspectives in Biology*. 5:a013334–a013334. doi:10.1101/cshperspect.a013334.

Deshaies, R.J., and R. Schekman. 1987. A yeast mutant defective at an early stage in import of secretory protein precursors into the endoplasmic reticulum. *J Cell Biol*. 105:633–645.

Dong, H., M. Sharma, H.-X. Zhou, and T.A. Cross. 2012. Glycines: Role in α-Helical Membrane Protein Structures and a Potential Indicator of Native Conformation. *Biochemistry*. 51:4779–4789. doi:10.1021/bi300090x.

Drozdetskiy, A., C. Cole, J. Procter, and G.J. Barton. 2015. JPred4: a protein secondary structure prediction server. *Nucleic Acids Res*. 43:W389–94. doi:10.1093/nar/gkv332.

Dufourc, E.J. 2008. Sterols and membrane dynamics. *J Chem Biol*. 1:63–77. doi:10.1007/s12154-008-0010-6.

Dunn, C.D., and R.E. Jensen. 2003. Suppression of a defect in mitochondrial protein import identifies cytosolic proteins required for viability of yeast cells lacking mitochondrial DNA. *Genetics*. 165:35–45.

Durfee, T., K. Becherer, P.L. Chen, S.H. Yeh, Y. Yang, A.E. Kilburn, W.H. Lee, and S.J. Elledge. 1993. The retinoblastoma protein associates with the protein phosphatase type 1 catalytic subunit. *Genes Dev*. 7:555–569. doi:10.1101/gad.7.4.555.

Edlich, F., S. Banerjee, M. Suzuki, M.M. Cleland, D. Arnoult, C. Wang, A. Neutzner, N. Tjandra, and R.J. Youle. 2011. Bcl-xL Retrotranslocates Bax from the Mitochondria into the Cytosol. *Cell*. 145:104–116. doi:10.1016/j.cell.2011.02.034.

Einerhand, A.W., T.M. Voorn-Brouwer, R. Erdmann, W.H. Kunau, and H.F. Tabak. 1991. Regulation of transcription of the gene coding for peroxisomal 3-oxoacyl-CoA thiolase of Saccharomcyes cerevisiae. *European Journal of Biochemistry*. 200:113–122. doi:10.1111/j.1432-1033.1991.tb21056.x.

Elazar, A., J. Weinstein, I. Biran, Y. Fridman, E. Bibi, and S.J. Fleishman. 2016. Mutational scanning reveals the determinants of protein insertion and association energetics in the plasma membrane. *eLife*. 5:1302. doi:10.7554/eLife.12125.

Engelman, D.M., and T.A. Steitz. 1981. The spontaneous insertion of proteins into and across membranes: the helical hairpin hypothesis. *Cell*. 23:411–422. doi:10.1016/0092-8674(81)90136-7.

Fekkes, P., K.A. Shepard, and M.P. Yaffe. 2000. Gag3p, an outer membrane protein required for fission of mitochondrial tubules. *J Cell Biol*. 151:333–340.

Fowler, D.M., and S. Fields. 2014. Deep mutational scanning: a new style of protein science. *Nature Publishing Group*. 11:801–807. doi:10.1038/nmeth.3027.

Förtsch, J., E. Hummel, M. Krist, and B. Westermann. 2011. The myosin-related motor protein Myo2 is an essential mediator of bud-directed mitochondrial movement in yeast. *J Cell Biol*. 194:473–488. doi:10.1083/jcb.201012088.

Garipler, G., N. Mutlu, N.A. Lack, and C.D. Dunn. 2014. Deletion of conserved protein phosphatases reverses defects associated with mitochondrial DNA damage in Saccharomyces cerevisiae. *Proceedings of the National Academy of Sciences*. 111:1473–1478. doi:10.1073/pnas.1312399111.

Gimpelev, M., L.R. Forrest, D. Murray, and B. Honig. 2004. Helical Packing Patterns in Membrane and Soluble Proteins. *Biophysical Journal*. 87:4075–4086.

Goecks, J., A. Nekrutenko, J. Taylor, Galaxy Team. 2010. Galaxy: a comprehensive approach for supporting accessible, reproducible, and transparent computational research in the life sciences. *Genome Biol*. 11:R86. doi:10.1186/gb-2010-11-8-r86.

Gross, A., K. Pilcher, E. Blachly-Dyson, E. Basso, J. Jockel, M.C. Bassik, S.J. Korsmeyer, and M. Forte. 2000. Biochemical and Genetic Analysis of the Mitochondrial Response of Yeast to BAX and BCL-XL. *Mol Cell Biol*. 20:3125–3136. doi:10.1128/MCB.20.9.3125-3136.2000.

Habib, S.J., A. Vasiljev, W. Neupert, and D. Rapaport. 2003. Multiple functions of tail-anchor domains of mitochondrial outer membrane proteins. *FEBS Lett*. 555:511–515. doi:10.1016/S0014-5793(03)01325-5.

He, S., and T.D. Fox. 1999. Mutations affecting a yeast mitochondrial inner membrane protein, pnt1p, block export of a mitochondrially synthesized fusion protein from the matrix. *Mol Cell Biol*. 19:6598–6607.

Hermann, G.J., J.W. Thatcher, J.P. Mills, K.G. Hales, M.T. Fuller, J. Nunnari, and J.M. Shaw. 1998. Mitochondrial fusion in yeast requires the transmembrane GTPase Fzo1p. *J Cell Biol*. 143:359–373.

Hietpas, R.T., J.D. Jensen, and D.N.A. Bolon. 2011. Experimental illumination of a fitness landscape. *Proceedings of the National Academy of Sciences*. 108:7896–7901. doi:10.1073/pnas.1016024108.

Honig, B.H., and W.L. Hubbell. 1984. Stability of “salt bridges” in membrane proteins. *Proc Natl Acad Sci USA*. 81:5412–5416.

Horie, C., H. Suzuki, M. Sakaguchi, and K. Mihara. 2002. Characterization of signal that directs C-tail-anchored proteins to mammalian mitochondrial outer membrane. *Mol Biol Cell*. 13:1615–1625. doi:10.1091/mbc.01-12-0570.

Horie, C., H. Suzuki, M. Sakaguchi, and K. Mihara. 2003. Targeting and assembly of mitochondrial tail-anchored protein Tom5 to the TOM complex depend on a signal distinct from that of tail-anchored proteins dispersed in the membrane. *J Biol Chem*. 278:41462–41471. doi:10.1074/jbc.M307047200.

Isenmann, S., Y. Khew-Goodall, J. Gamble, M. Vadas, and B.W. Wattenberg. 1998. A splice-isoform of vesicle-associated membrane protein-1 (VAMP-1) contains a mitochondrial targeting signal. *Mol Biol Cell*. 9:1649–1660.

Jensen, R.E., S. Schmidt, and R.J. Mark. 1992. Mutations in a 19-amino-acid hydrophobic region of the yeast cytochrome c1 presequence prevent sorting to the mitochondrial intermembrane space. *Mol Cell Biol*. 12:4677–4686.

Johnson, N., K. Powis, and S. High. 2013. Post-translational translocation into the endoplasmic reticulum. *BBA-Molecular Cell Research*. 1833:2403–2409. doi:10.1016/j.bbamcr.2012.12.008.

Kemper, C., S.J. Habib, G. Engl, P. Heckmeyer, K.S. Dimmer, and D. Rapaport. 2008. Integration of tail-anchored proteins into the mitochondrial outer membrane does not require any known import components. *Journal of Cell Science*. 121:1990–1998. doi:10.1242/jcs.024034.

Kim, C., T. Schmidt, E.-G. Cho, F. Ye, T.S. Ulmer, and M.H. Ginsberg. 2012. Basic amino-acid side chains regulate transmembrane integrin signalling. *Nature*. 481:209–213. doi:10.1038/nature10697.

Klecker, T., M. Wemmer, M. Haag, A. Weig, S. Böckler, T. Langer, J. Nunnari, and B. Westermann. 2015. Interaction of MDM33 with mitochondrial inner membrane homeostasis pathways in yeast. *Sci. Rep.* 1–14. doi:10.1038/srep18344.

Koch, A., Y. Yoon, N.A. Bonekamp, M.A. McNiven, and M. Schrader. 2005. A role for Fis1 in both mitochondrial and peroxisomal fission in mammalian cells. *Mol Biol Cell*. 16:5077–5086. doi:10.1091/mbc.E05-02-0159.

Krumpe, K., I. Frumkin, Y. Herzig, N. Rimon, C. Özbalci, B. Brügger, D. Rapaport, and M. Schuldiner. 2012. Ergosterol content specifies targeting of tail-anchored proteins to mitochondrial outer membranes. *Mol Biol Cell*. 23:3927–3935. doi:10.1091/mbc.E11-12-0994.

Kuravi, K., S. Nagotu, A.M. Krikken, K. Sjollema, M. Deckers, R. Erdmann, M. Veenhuis, and I.J. van der Klei. 2006. Dynamin-related proteins Vps1p and Dnm1p control peroxisome abundance in Saccharomyces cerevisiae. *Journal of Cell Science*. 119:3994–4001. doi:10.1242/jcs.03166.

Kuroda, R., T. Ikenoue, M. Honsho, S. Tsujimoto, J.Y. Mitoma, and A. Ito. 1998. Charged amino acids at the carboxyl-terminal portions determine the intracellular locations of two isoforms of cytochrome b5. *J Biol Chem*. 273:31097–31102.

Lee, J., D.H. Kim, and I. Hwang. 2014. Specific targeting of proteins to outer envelope membranes of endosymbiotic organelles, chloroplasts, and mitochondria. *Front Plant Sci*. 5:173. doi:10.3389/fpls.2014.00173.

Lee, S., W.A. Lim, and K.S. Thorn. 2013. Improved blue, green, and red fluorescent protein tagging vectors for S. cerevisiae. *PLoS ONE*. 8:e67902. doi:10.1371/journal.pone.0067902.

Li, S.C., N.K. Goto, K.A. Williams, and C.M. Deber. 1996. Alpha-helical, but not beta-sheet, propensity of proline is determined by peptide environment. *Proc Natl Acad Sci USA*. 93:6676–6681.

Long, S.B., E.B. Campbell, and R. MacKinnon. 2005. Voltage Sensor of Kv1.2: Structural Basis of Electromechanical Coupling. *Science*. 309:903–908. doi:10.1126/science.1116270.

Maarse, A.C., J. Blom, L.A. Grivell, and M. Meijer. 1992. MPI1, an essential gene encoding a mitochondrial membrane protein, is possibly involved in protein import into yeast mitochondria. *EMBO J*. 11:3619–3628.

Masella, A.P., A.K. Bartram, J.M. Truszkowski, D.G. Brown, and J.D. Neufeld. 2012. PANDAseq: paired-end assembler for illumina sequences. *BMC Bioinformatics*. 13:31. doi:10.1186/1471-2105-13-31.

Melamed, D., D.L. Young, C.E. Gamble, C.R. Miller, and S. Fields. 2013. Deep mutational scanning of an RRM domain of the Saccharomyces cerevisiae poly(A)-binding protein. *RNA*. 19:1537–1551. doi:10.1261/rna.040709.113.

Meyers, S., W. Schauer, E. Balzi, M. Wagner, A. Goffeau, and J. Golin. 1992. Interaction of the yeast pleiotropic drug resistance genes PDR1 and PDR5. *Curr Genet*. 21:431–436. doi:10.1007/BF00351651.

Monné, M., I. Nilsson, M. Johansson, N. Elmhed, and G. von Heijne. 1998. Positively and negatively charged residues have different effects on the position in the membrane of a model transmembrane helix. *J Mol Biol*. 284:1177–1183. doi:10.1006/jmbi.1998.2218.

Mozdy, A.D., J.M. McCaffery, and J.M. Shaw. 2000. Dnm1p GTPase-mediated mitochondrial fission is a multi-step process requiring the novel integral membrane component Fis1p. *J Cell Biol*. 151:367–380.

Mutlu, N., G. Garipler, E. Akdoğan, and C.D. Dunn. 2014. Activation of the pleiotropic drug resistance pathway can promote mitochondrial DNA retention by fusion-defective mitochondria in Saccharomyces cerevisiae. *G3 (Bethesda)*. 4:1247–1258. doi:10.1534/g3.114.010330.

Nechushtan, A., C.L. Smith, Y.T. Hsu, and R.J. Youle. 1999. Conformation of the Bax C-terminus regulates subcellular location and cell death. *EMBO J*. 18:2330–2341. doi:10.1093/emboj/18.9.2330.

Neupert, W. 2015. A Perspective on Transport of Proteins into Mitochondria: A Myriad of Open Questions. *J Mol Biol*. 427:1135–1158. doi:10.1016/j.jmb.2015.02.001.

O'Neil, K.T., and W.F. DeGrado. 1990. A thermodynamic scale for the helix-forming tendencies of the commonly occurring amino acids. *Science*. 250:646–651.

Okreglak, V., and P. Walter. 2014. The conserved AAA-ATPase Msp1 confers organelle specificity to tail-anchored proteins. *Proceedings of the National Academy of Sciences*. 111:8019–8024. doi:10.1073/pnas.1405755111.

Oldenburg, K.R., K.T. Vo, S. Michaelis, and C. Paddon. 1997. Recombination-mediated PCR-directed plasmid construction in vivo in yeast. *Nucleic Acids Res*. 25:451–452.

Ott, M., E. Norberg, K.M. Walter, P. Schreiner, C. Kemper, D. Rapaport, B. Zhivotovsky, and S. Orrenius. 2007. The mitochondrial TOM complex is required for tBid/Bax-induced cytochrome c release. *J Biol Chem*. 282:27633–27639. doi:10.1074/jbc.M703155200.

Parsegian, A. 1969. Energy of an ion crossing a low dielectric membrane: solutions to four relevant electrostatic problems. *Nature*. 221:844–846. doi:10.1038/221844a0.

Pavlidis, P., and W.S. Noble. 2003. Matrix2png: a utility for visualizing matrix data. *Bioinformatics*. 19:295–296.

Prasad, R., and A. Goffeau. 2012. Yeast ATP-Binding Cassette Transporters Conferring Multidrug Resistance. *Annu. Rev. Microbiol.* 66:39–63. doi:10.1146/annurev-micro-092611-150111.

Rapaport, D. 2003. Finding the right organelle. Targeting signals in mitochondrial outer-membrane proteins. *EMBO Rep*. 4:948–952. doi:10.1038/sj.embor.embor937.

Rapaport, D., M. Brunner, W. Neupert, and B. Westermann. 1998. Fzo1p is a mitochondrial outer membrane protein essential for the biogenesis of functional mitochondria in Saccharomyces cerevisiae. *J Biol Chem*. 273:20150–20155.

Robinson, J.S., D.J. Klionsky, L.M. Banta, and S.D. Emr. 1988. Protein sorting in Saccharomyces cerevisiae: isolation of mutants defective in the delivery and processing of multiple vacuolar hydrolases. *Mol Cell Biol*. 8:4936–4948. doi:10.1128/MCB.8.11.4936.

Russ, W.P., and D.M. Engelman. 2000. The GxxxG motif: A framework for transmembrane helix-helix association. *J Mol Biol*. 296:911–919.

Ryan, K.R., R.S. Leung, and R.E. Jensen. 1998. Characterization of the mitochondrial inner membrane translocase complex: the Tim23p hydrophobic domain interacts with Tim17p but not with other Tim23p molecules. *Mol Cell*

Biol. 18:178–187.

Sapay, N., Y. Guermeur, and G. Deléage. 2006. BMC Bioinformatics. *BMC Bioinformatics*. 7:255–11. doi:10.1186/1471-2105-7-255.

Schellenberg, B., P. Wang, J.A. Keeble, R. Rodriguez-Enriquez, S. Walker, T.W. Owens, F. Foster, J. Tanianis-Hughes, K. Brennan, C.H. Streuli, and A.P. Gilmore. 2013. Bax Exists in a Dynamic Equilibrium between the Cytosol and Mitochondria to Control Apoptotic Priming. *Molecular Cell*. 49:959–971. doi:10.1016/j.molcel.2012.12.022.

Schinzel, A., T. Kaufmann, M. Schuler, J. Martinalbo, D. Grubb, and C. Borner. 2004. Conformational control of Bax localization and apoptotic activity by Pro168. *J Cell Biol*. 164:1021–1032. doi:10.1083/jcb.200309013.

Schow, E.V., J.A. Freites, P. Cheng, A. Bernsel, G. von Heijne, S.H. White, and D.J. Tobias. 2010. Arginine in Membranes: The Connection Between Molecular Dynamics Simulations and Translocon-Mediated Insertion Experiments. *J Membrane Biol*. 239:35–48. doi:10.1007/s00232-010-9330-x.

Schuldiner, M., J. Metz, V. Schmid, V. Denic, M. Rakwalska, H.D. Schmitt, B. Schwappach, and J.S. Weissman. 2008. The GET Complex Mediates Insertion of Tail-Anchored Proteins into the ER Membrane. *Cell*. 134:634–645. doi:10.1016/j.cell.2008.06.025.

Segrest, J.P., H. De Loof, J.G. Dohlman, C.G. Brouillette, and G.M. Anantharamaiah. 1990. Amphipathic helix motif: Classes and properties. *Proteins: Structure, Function, and Bioinformatics*. 8:103–117. doi:10.1002/prot.340080202.

Senes, A., D.E. Engel, and W.F. DeGrado. 2004. Folding of helical membrane proteins: the role of polar, GxxxG-like and proline motifs. *Current Opinion in Structural Biology*. 14:465–479. doi:10.1016/j.sbi.2004.07.007.

Sesaki, H., and R.E. Jensen. 1999. Division versus fusion: Dnm1p and Fzo1p antagonistically regulate mitochondrial shape. *J Cell Biol*. 147:699–706.

Setoguchi, K., H. Otera, and K. Mihara. 2006. Cytosolic factor- and TOM-independent import of C-tail-anchored mitochondrial outer membrane proteins. *EMBO J*. 25:5635–5647. doi:10.1038/sj.emboj.7601438.

Sikorski, R.S., and P. Hieter. 1989. A system of shuttle vectors and yeast host strains designed for efficient manipulation of DNA in Saccharomyces cerevisiae. *Genetics*. 122:19–27.

Starita, L.M., D.L. Young, M. Islam, J.O. Kitzman, J. Gullingsrud, R.J. Hause, D.M. Fowler, J.D. Parvin, J. Shendure, and S. Fields. 2015. Massively Parallel Functional Analysis of BRCA1 RING Domain Variants. *Genetics*. 200:413–422. doi:10.1534/genetics.115.175802.

Stirling, C.J., J. Rothblatt, M. Hosobuchi, R. Deshaies, and R. Schekman. 1992. Protein translocation mutants defective in the insertion of integral membrane proteins into the endoplasmic reticulum. *Mol Biol Cell*. 3:129–142.

Stojanovski, D., O.S. Koutsopoulos, K. Okamoto, and M.T. Ryan. 2004. Levels of human Fis1 at the mitochondrial outer membrane regulate mitochondrial morphology. *Journal of Cell Science*. 117:1201–1210. doi:10.1242/jcs.01058.

Strandberg, E., and J.A. Killian. 2003. Snorkeling of lysine side chains in transmembrane helices: how easy can it get? *FEBS Lett*. 544:69–73. doi:10.1016/S0014-5793(03)00475-7.

Suzuki, M., S.Y. Jeong, M. Karbowski, R.J. Youle, and N. Tjandra. 2003. The solution structure of human mitochondria fission protein Fis1 reveals a novel TPR-like helix bundle. *J Mol Biol*. 334:445–458.

Taxis, C., and M. Knop. 2006. System of centromeric, episomal, and integrative vectors based on drug resistance markers for Saccharomyces cerevisiae. 40. 6 pp.

Tieu, Q., and J. Nunnari. 2000. Mdv1p is a WD repeat protein that interacts with the dynamin-related GTPase, Dnm1p, to trigger mitochondrial division. *J Cell Biol*. 151:353–366.

Van der Leij, I., M.M. Franse, Y. Elgersma, B. Distel, and H.F. Tabak. 1993. PAS10 is a tetratricopeptide-repeat protein that is essential for the import of most matrix proteins into peroxisomes of Saccharomyces cerevisiae. *Proc Natl Acad Sci USA*. 90:11782–11786.

Vidal, M., P. Braun, E. Chen, J.D. Boeke, and E. Harlow. 1996a. Genetic characterization of a mammalian protein-protein interaction domain by using a yeast reverse two-hybrid system. *Proc Natl Acad Sci USA*. 93:10321–10326.

Vidal, M., R.K. Brachmann, A. Fattaey, E. Harlow, and J.D. Boeke. 1996b. Reverse two-hybrid and one-hybrid systems to detect dissociation of protein-protein and DNA-protein interactions. *Proc Natl Acad Sci USA*. 93:10315–10320.

Voss, N.R., M. Gerstein, T.A. Steitz, and P.B. Moore. 2006. The Geometry of the Ribosomal Polypeptide Exit Tunnel. *J Mol Biol*. 360:893–906. doi:10.1016/j.jmb.2006.05.023.

Wattenberg, B., and T. Lithgow. 2001. Targeting of C-terminal (tail)-anchored proteins: understanding how cytoplasmic activities are anchored to intracellular membranes. *Traffic*. 2:66–71.

Wells, R.C., and R.B. Hill. 2011. The cytosolic domain of Fis1 binds and reversibly clusters lipid vesicles. *PLoS ONE*. 6:e21384. doi:10.1371/journal.pone.0021384.

Yoon, Y., E.W. Krueger, B.J. Oswald, and M.A. McNiven. 2003. The mitochondrial protein hFis1 regulates mitochondrial fission in mammalian cells through an

interaction with the dynamin-like protein DLP1. *Mol Cell Biol*. 23:5409–5420. doi:10.1128/MCB.23.15.5409-5420.2003.

Yu, C.-H., Y. Dang, Z. Zhou, C. Wu, F. Zhao, M.S. Sachs, and Y. Liu. 2015. Codon Usage Influences the Local Rate of Translation Elongation to Regulate Co-translational Protein Folding. *Molecular Cell*. 59:744–754. doi:10.1016/j.molcel.2015.07.018.

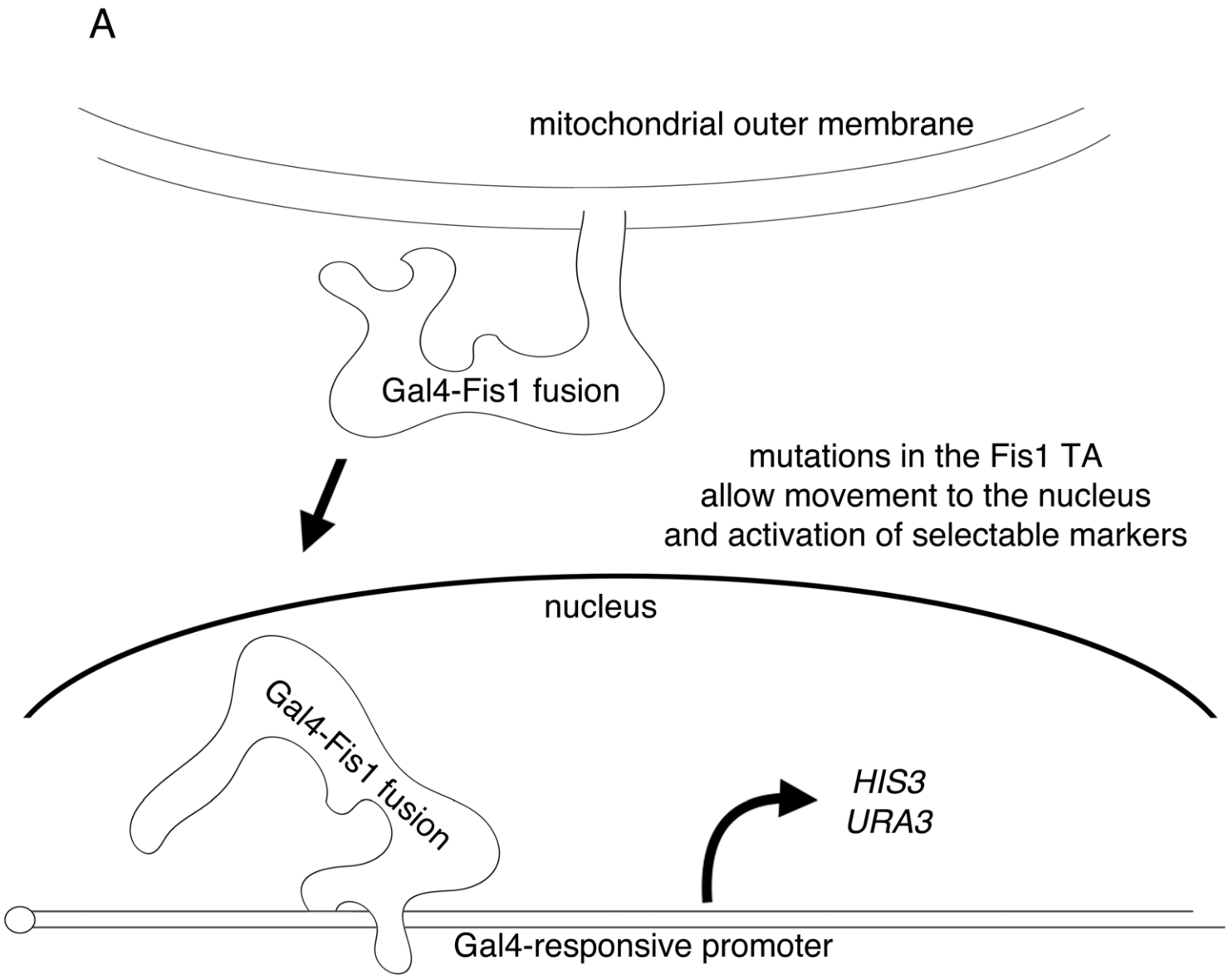

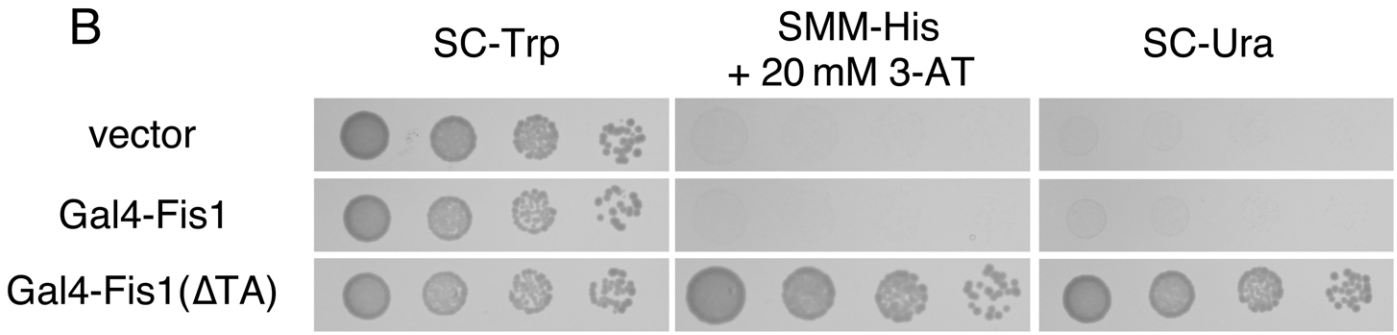

Figure 1

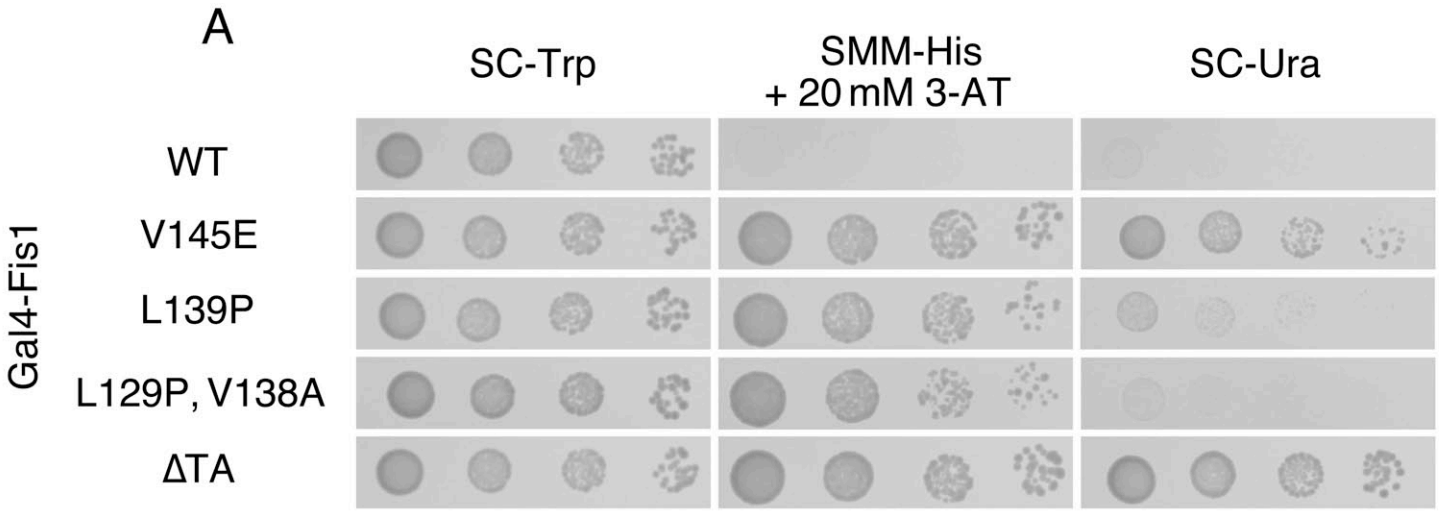

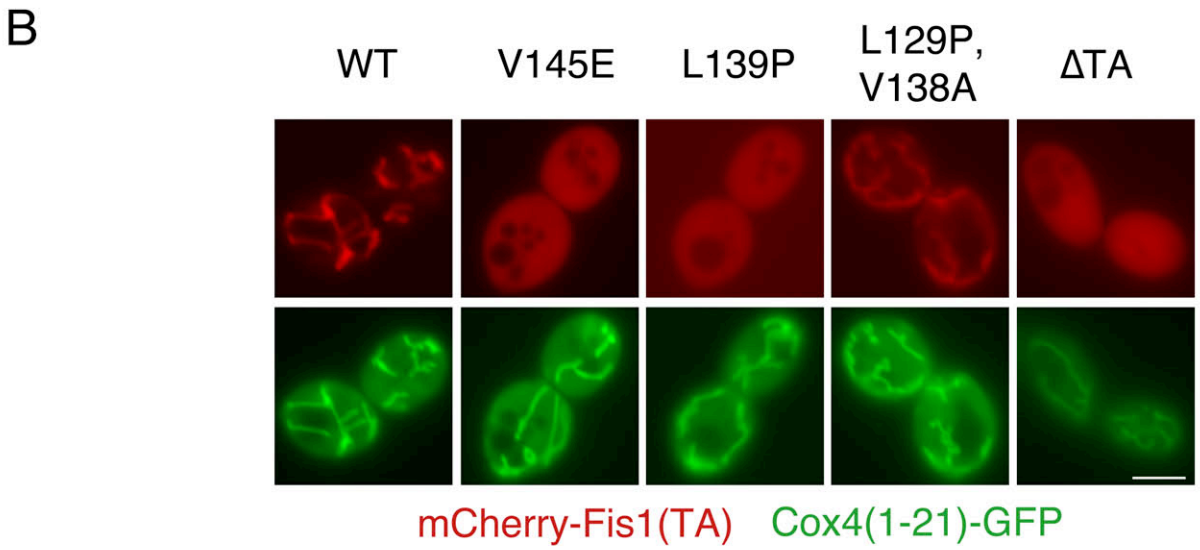

Figure 2

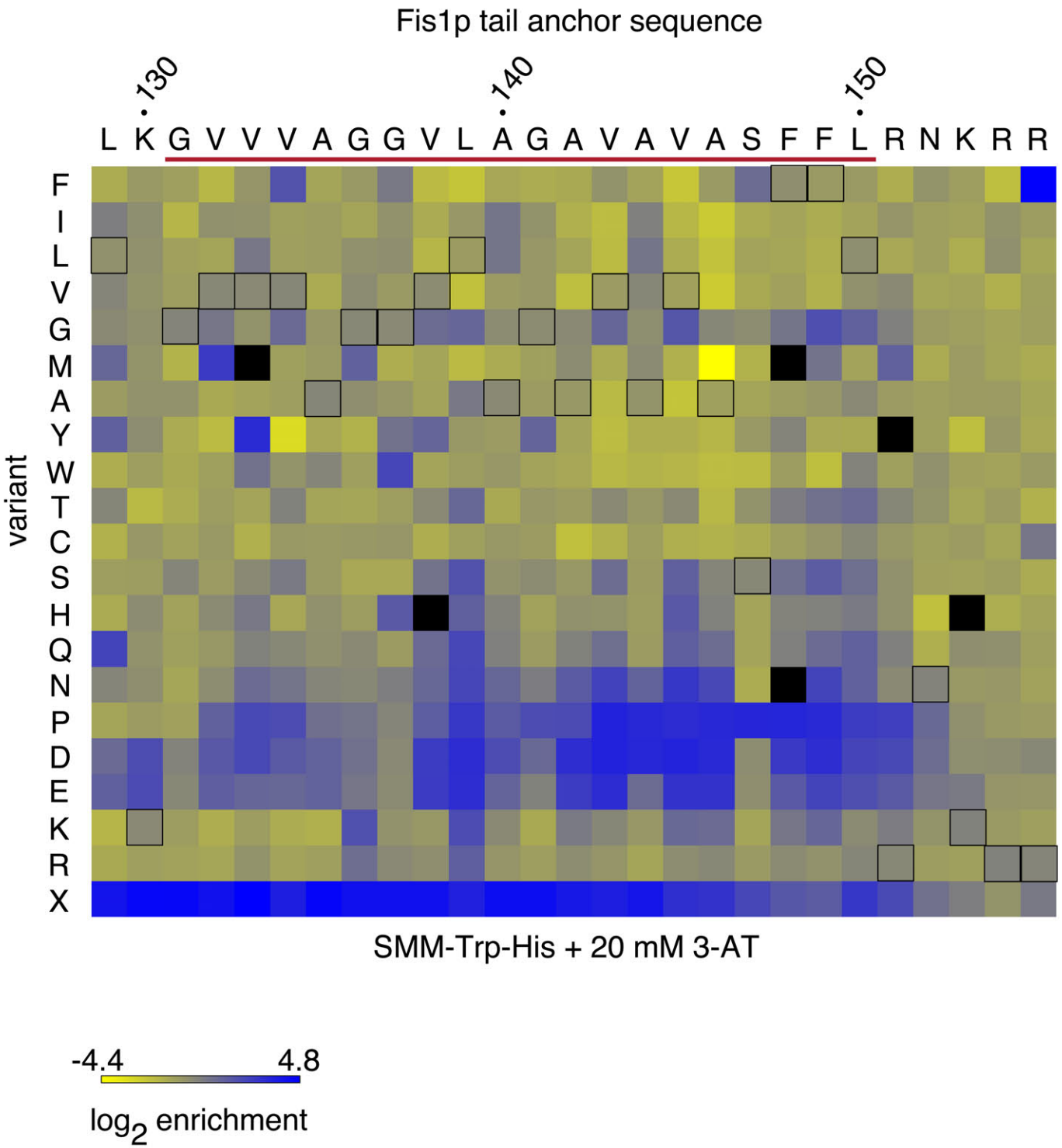

Figure 3

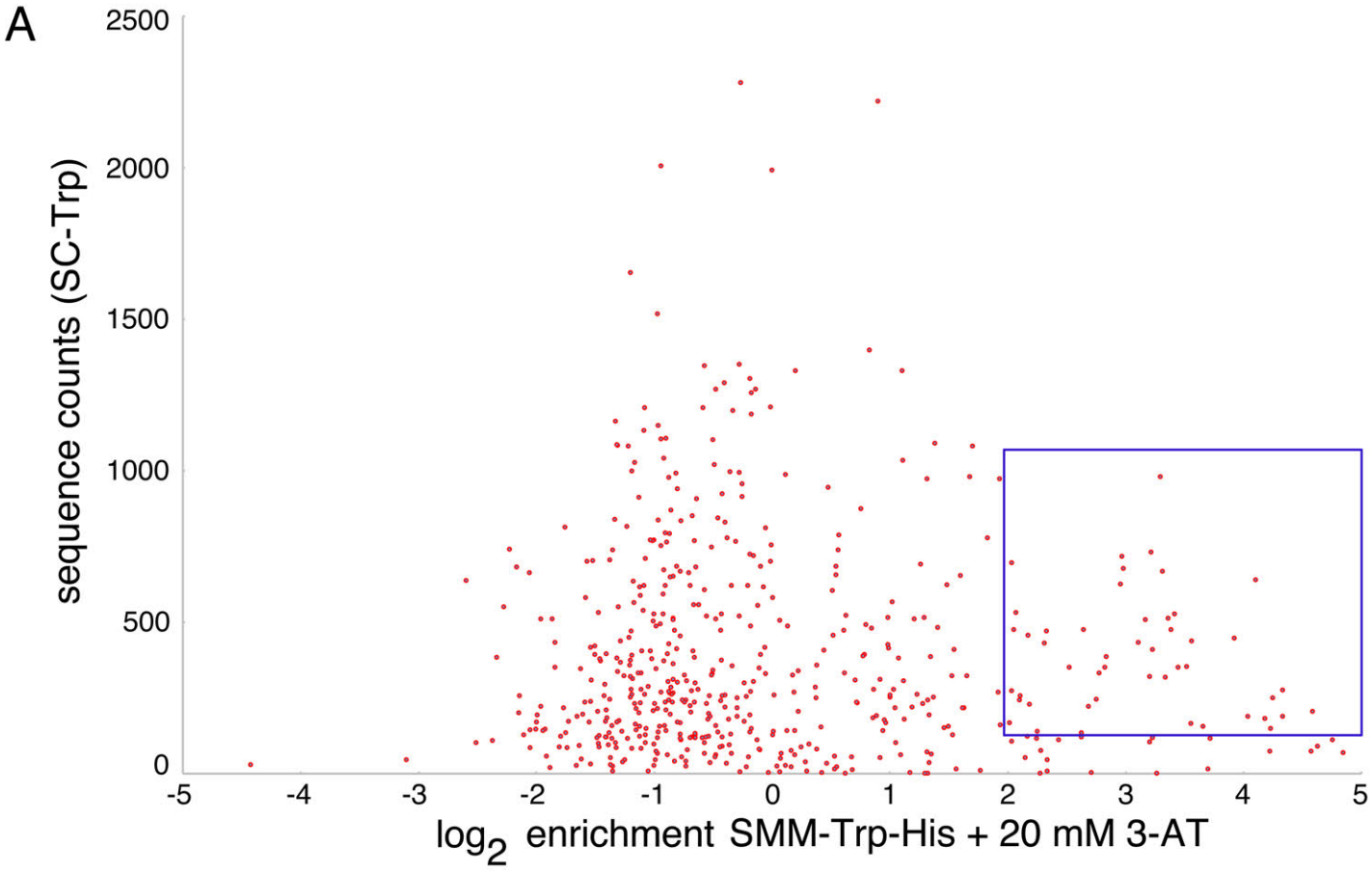

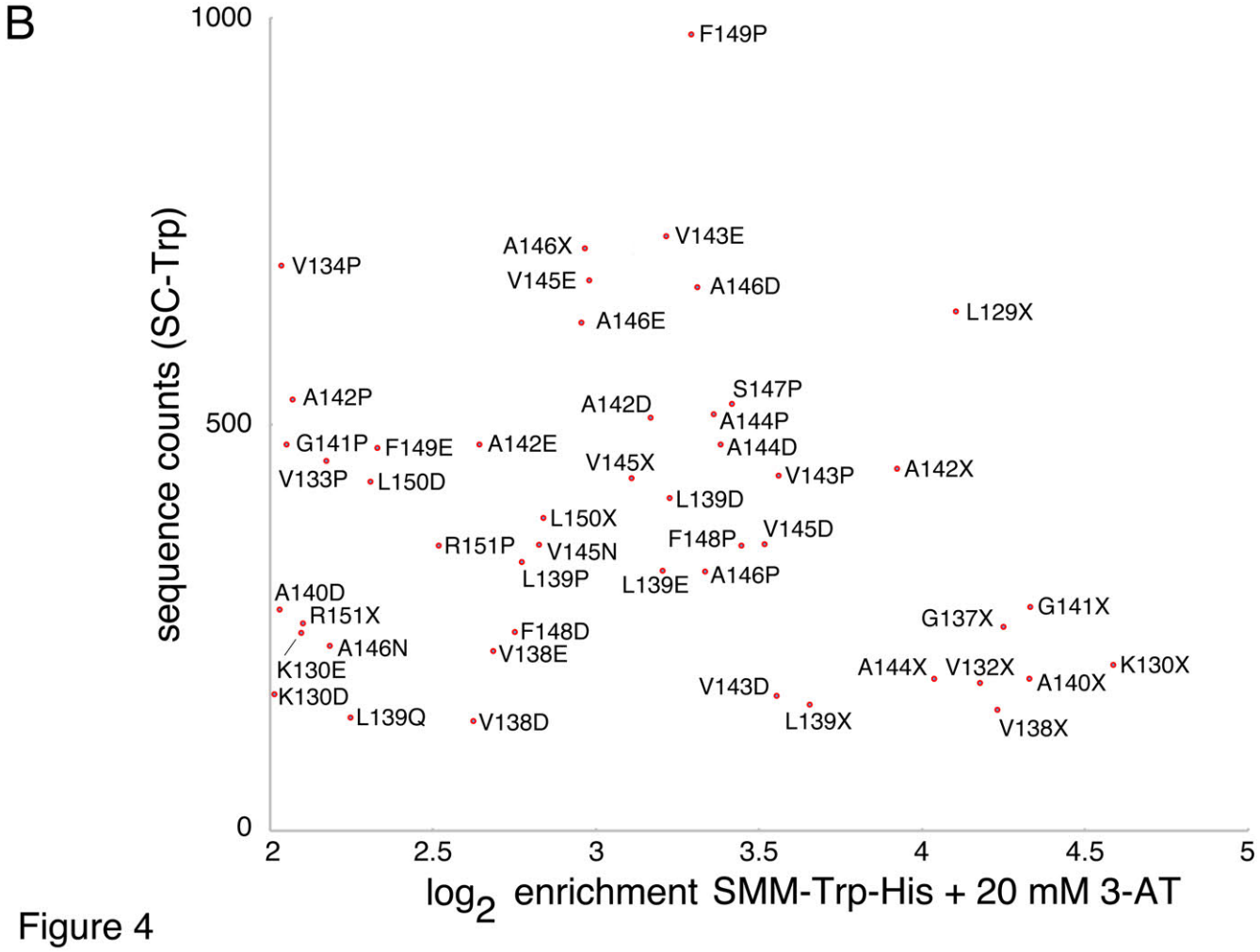

Figure 4

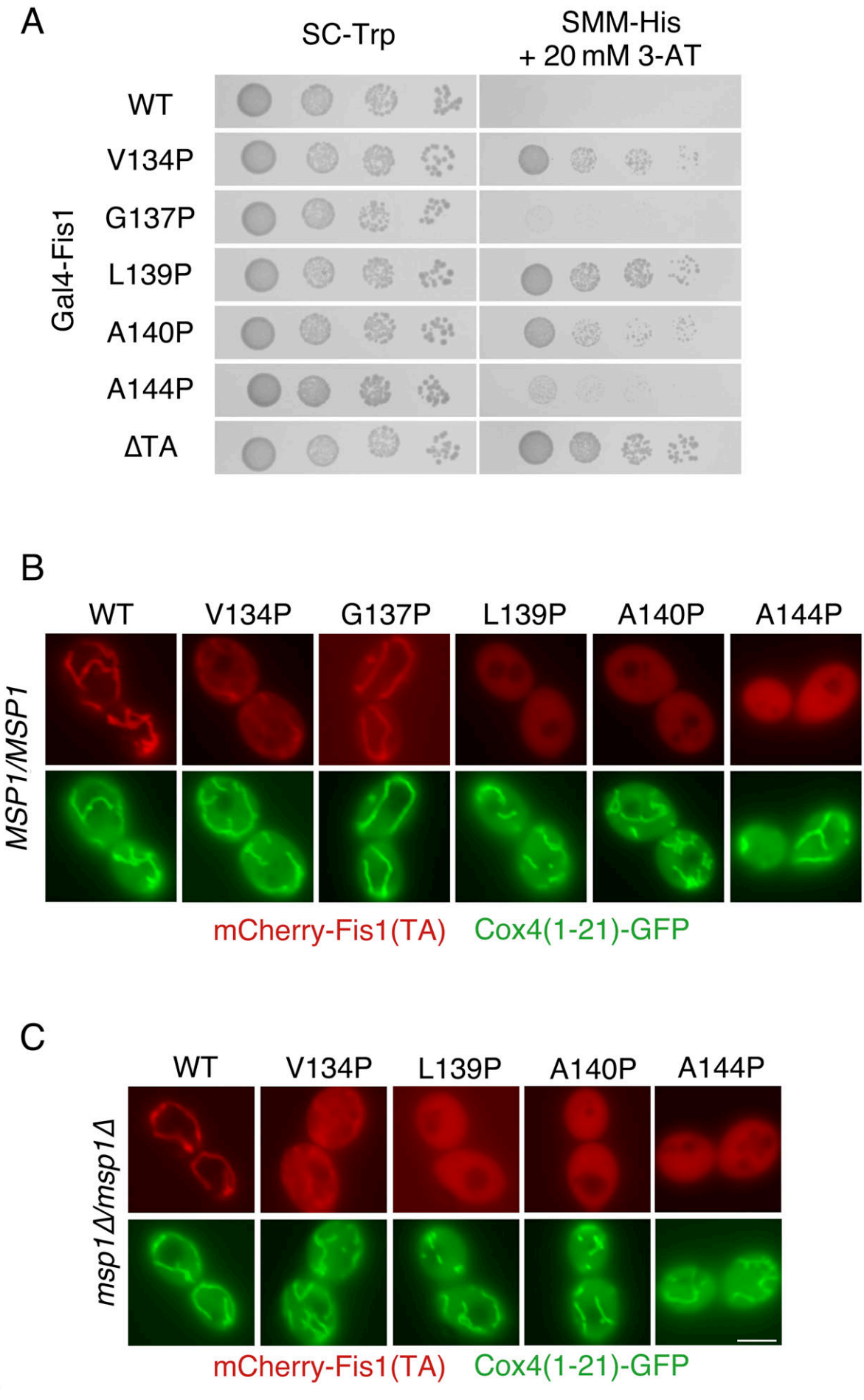

Figure 5

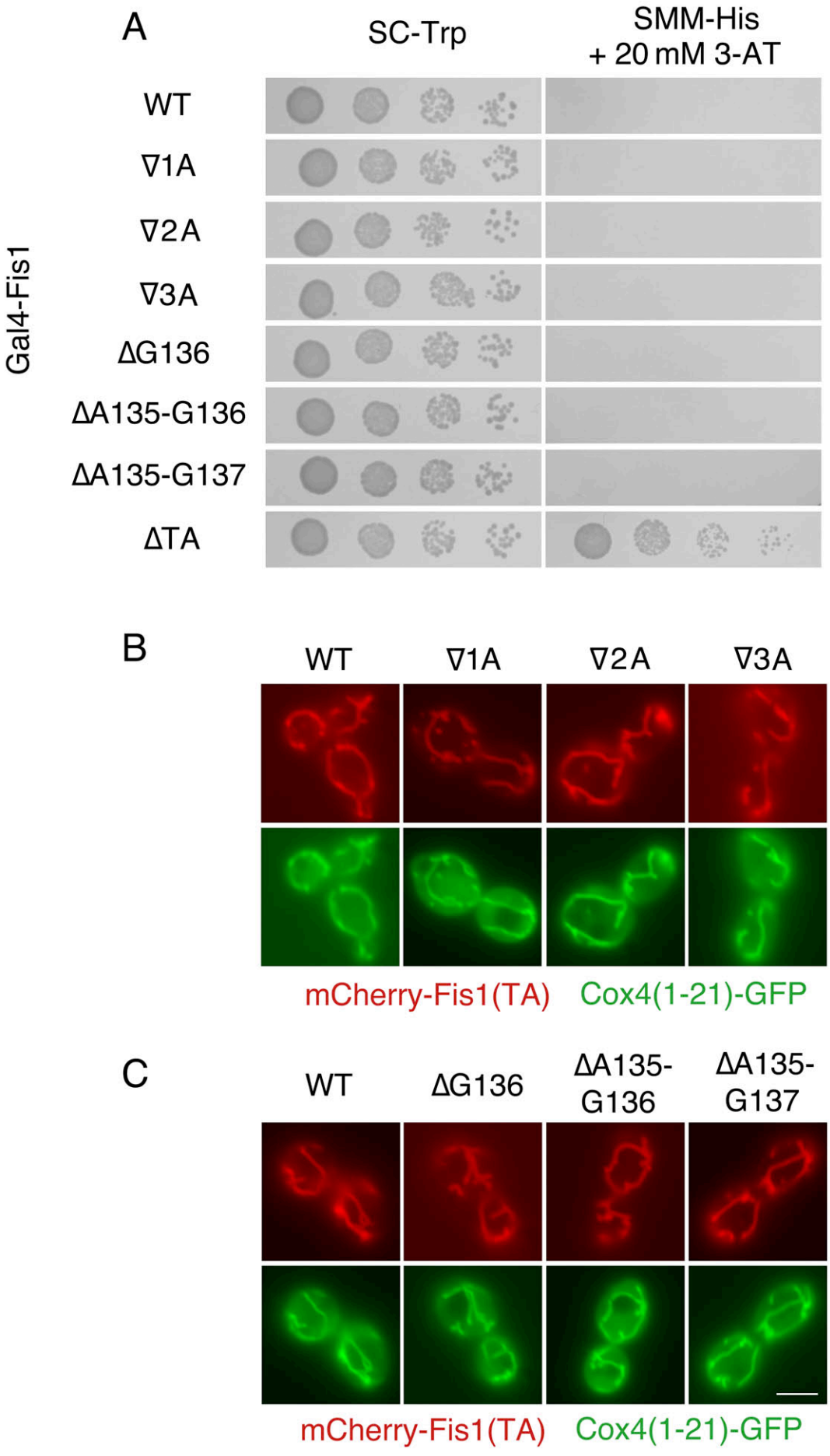

Figure 6

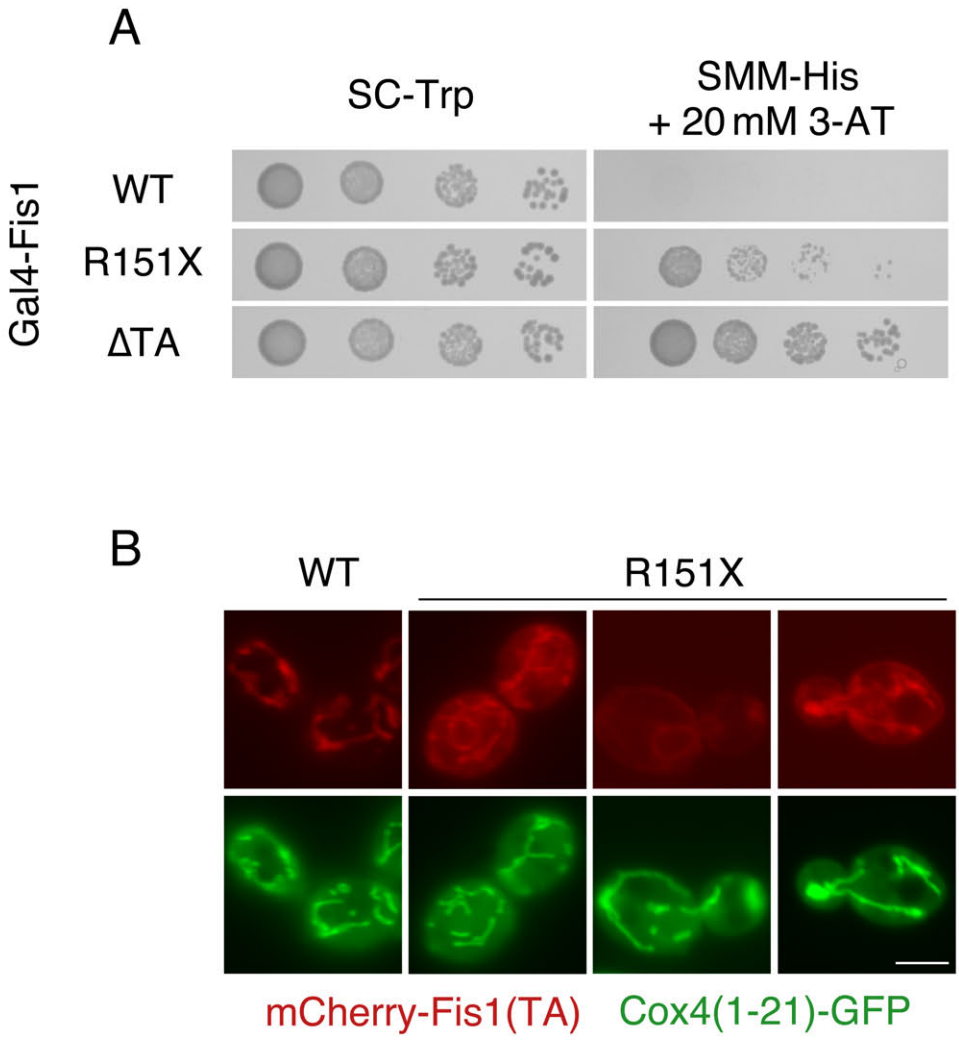

Figure 7

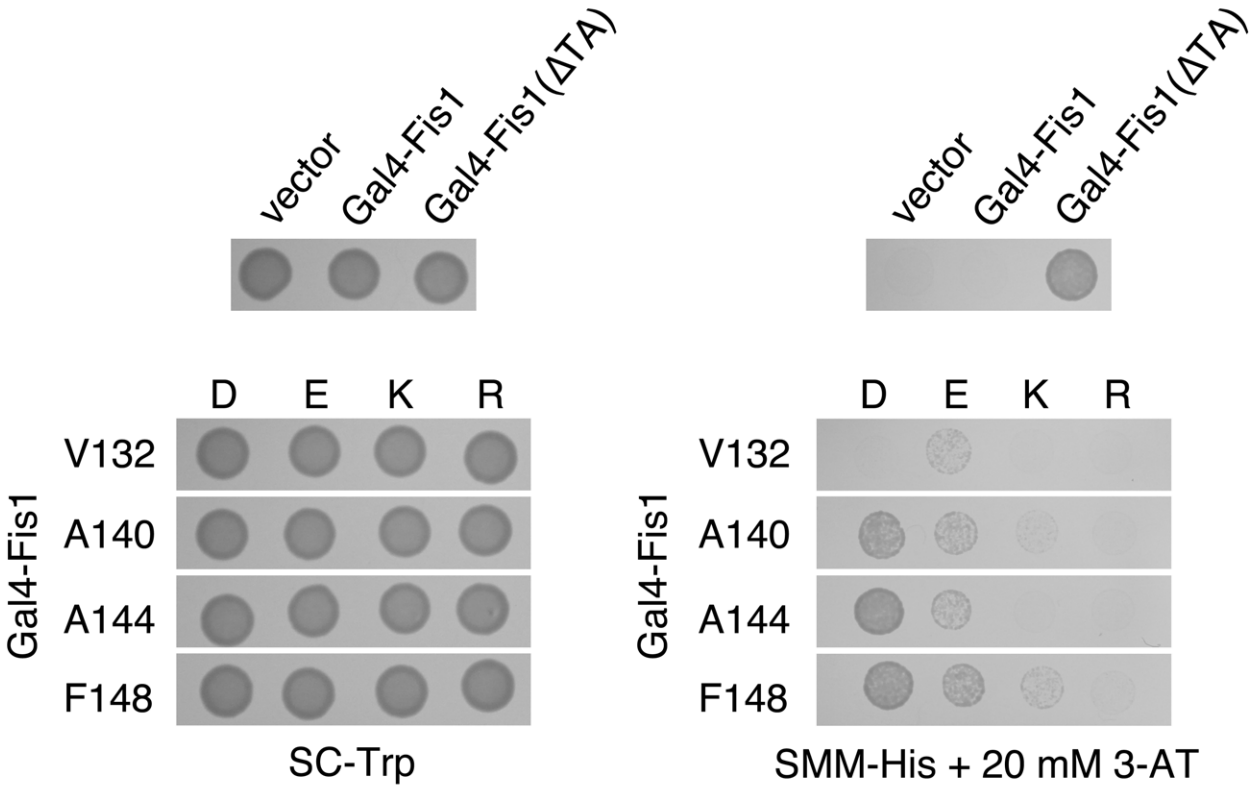

Figure 8

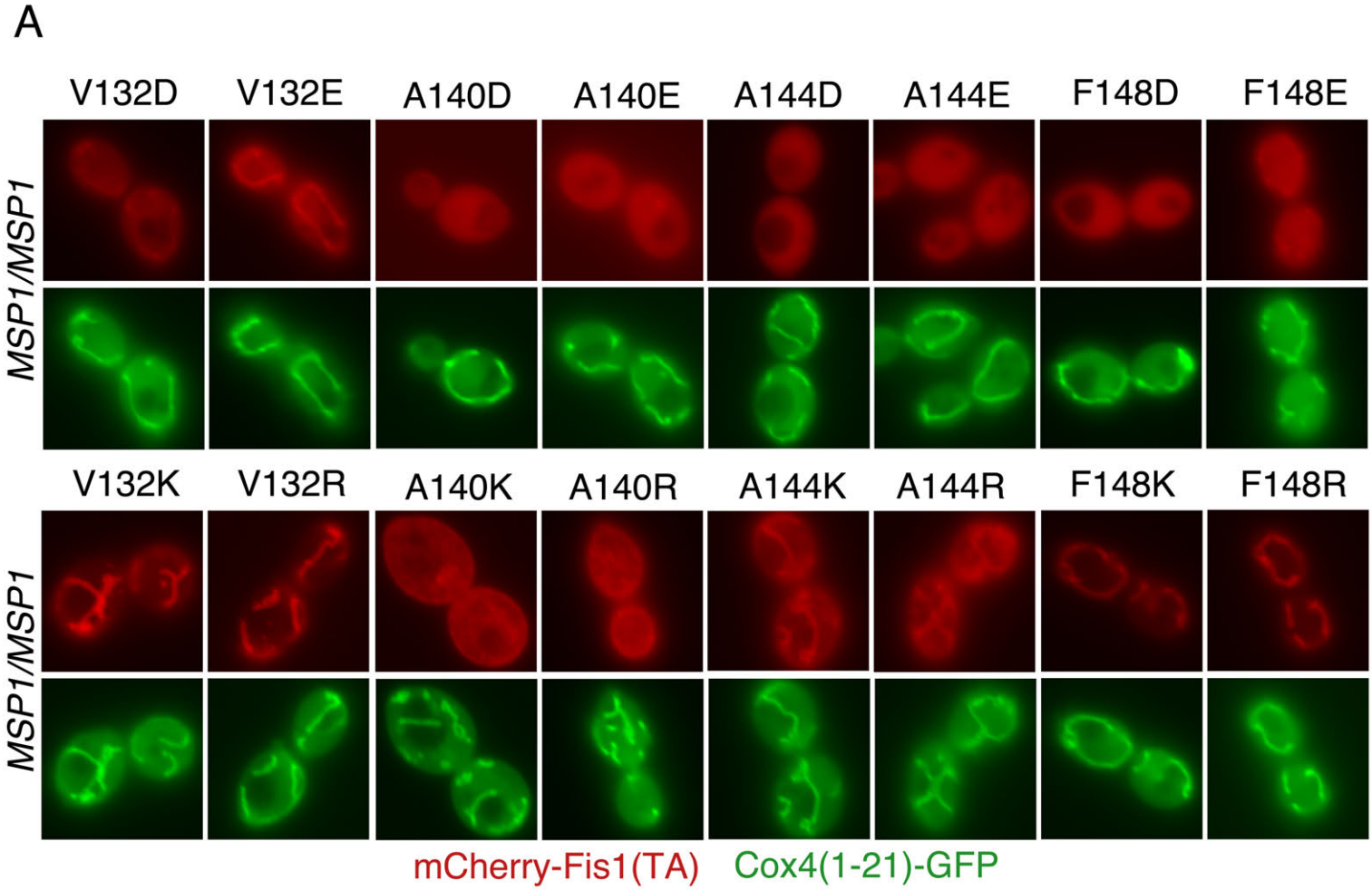

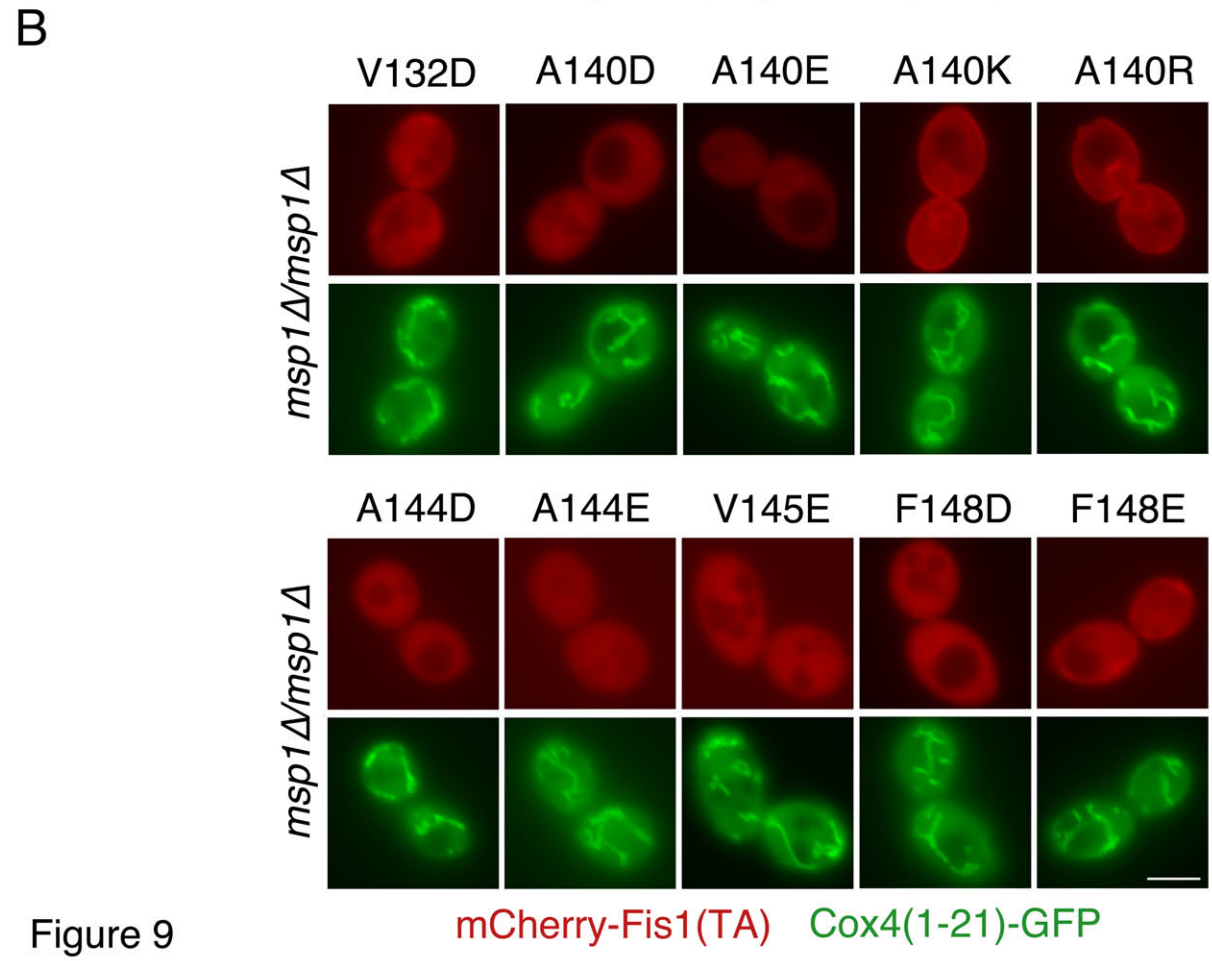

Figure 9

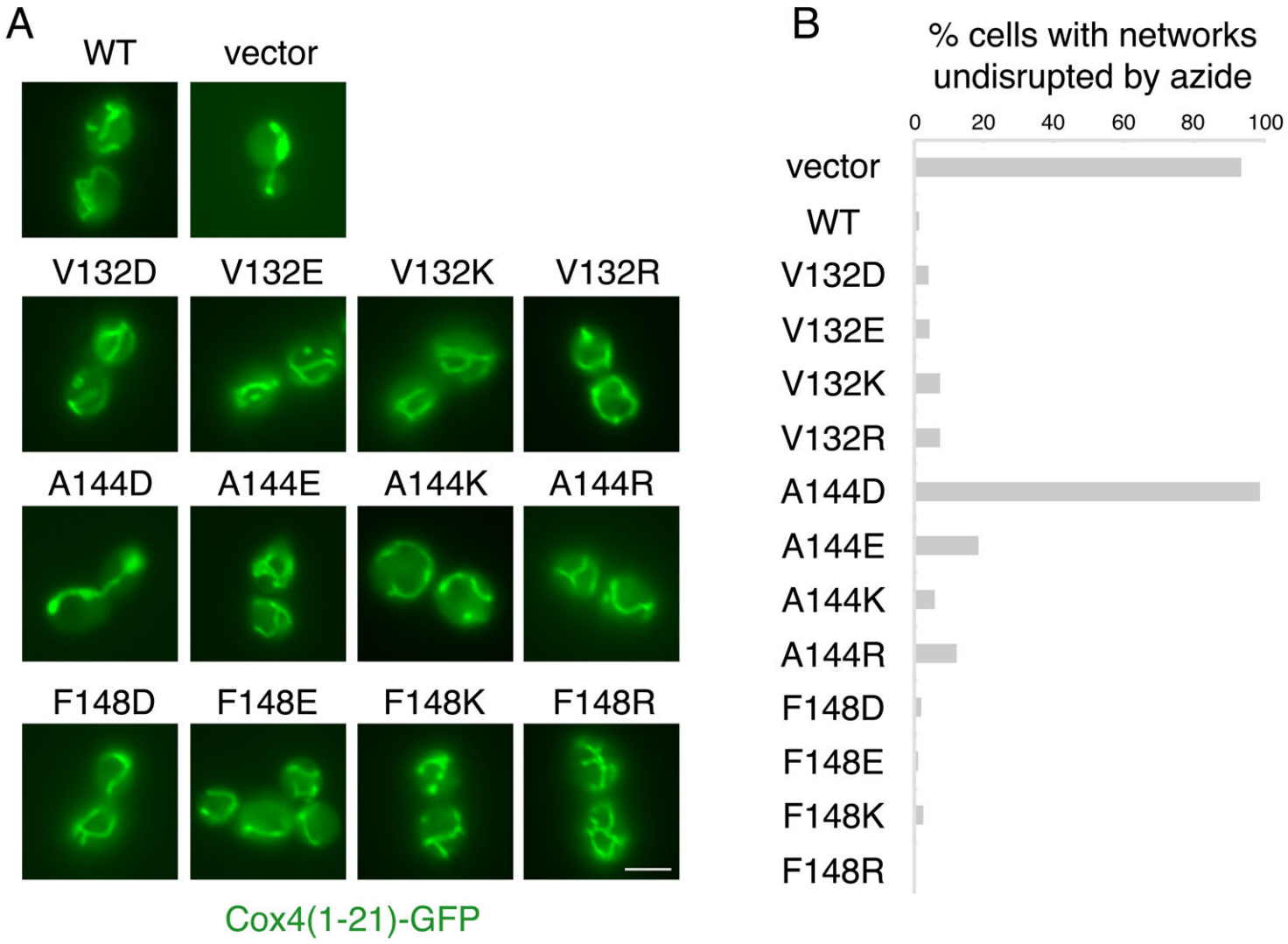

Figure 10

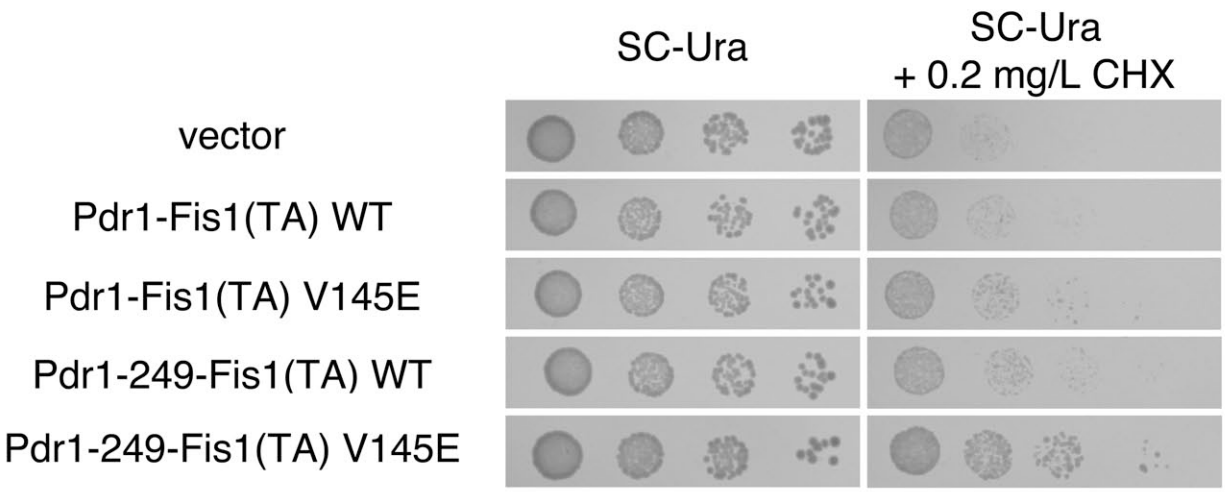

Figure S1

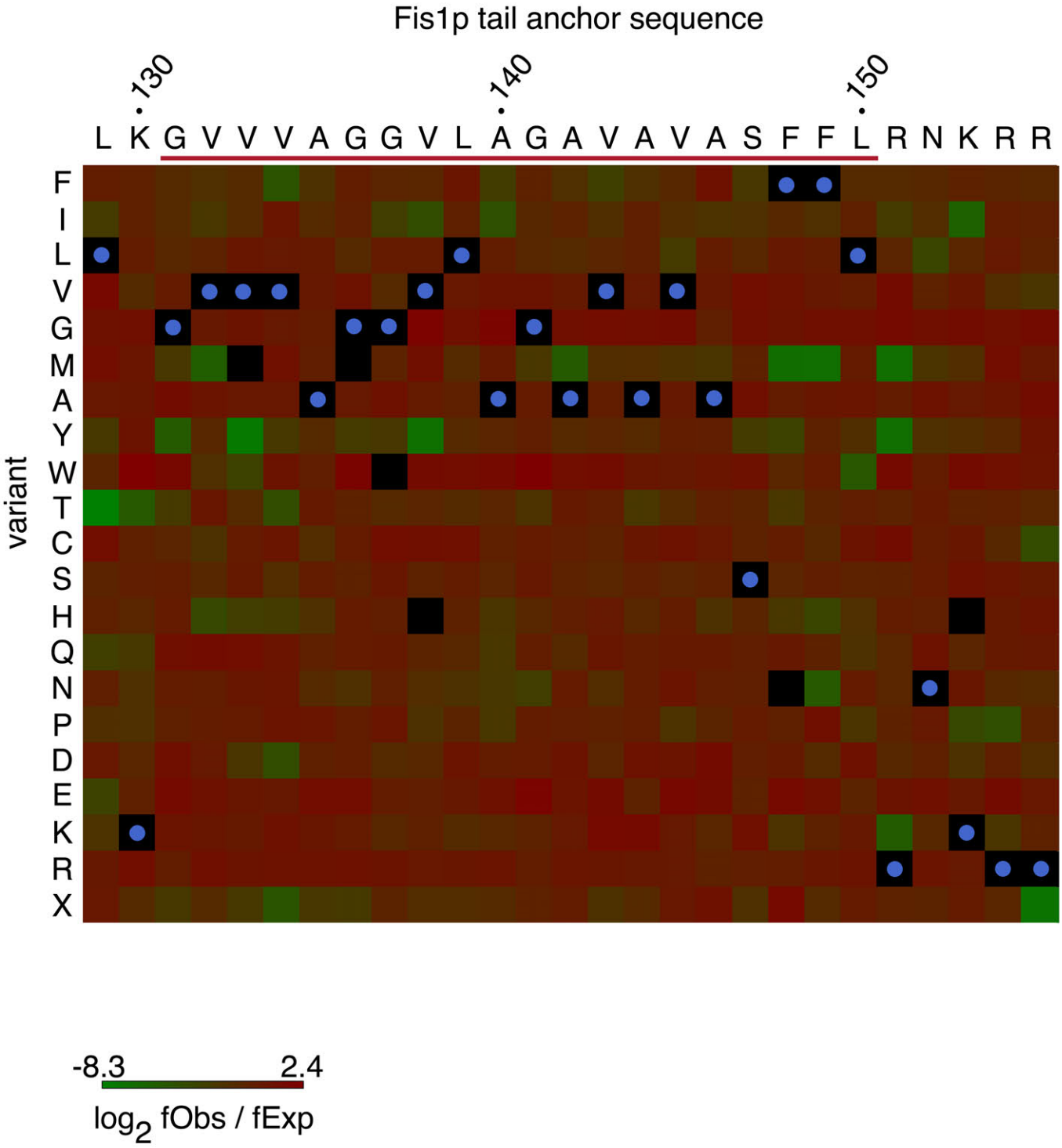

Figure S2

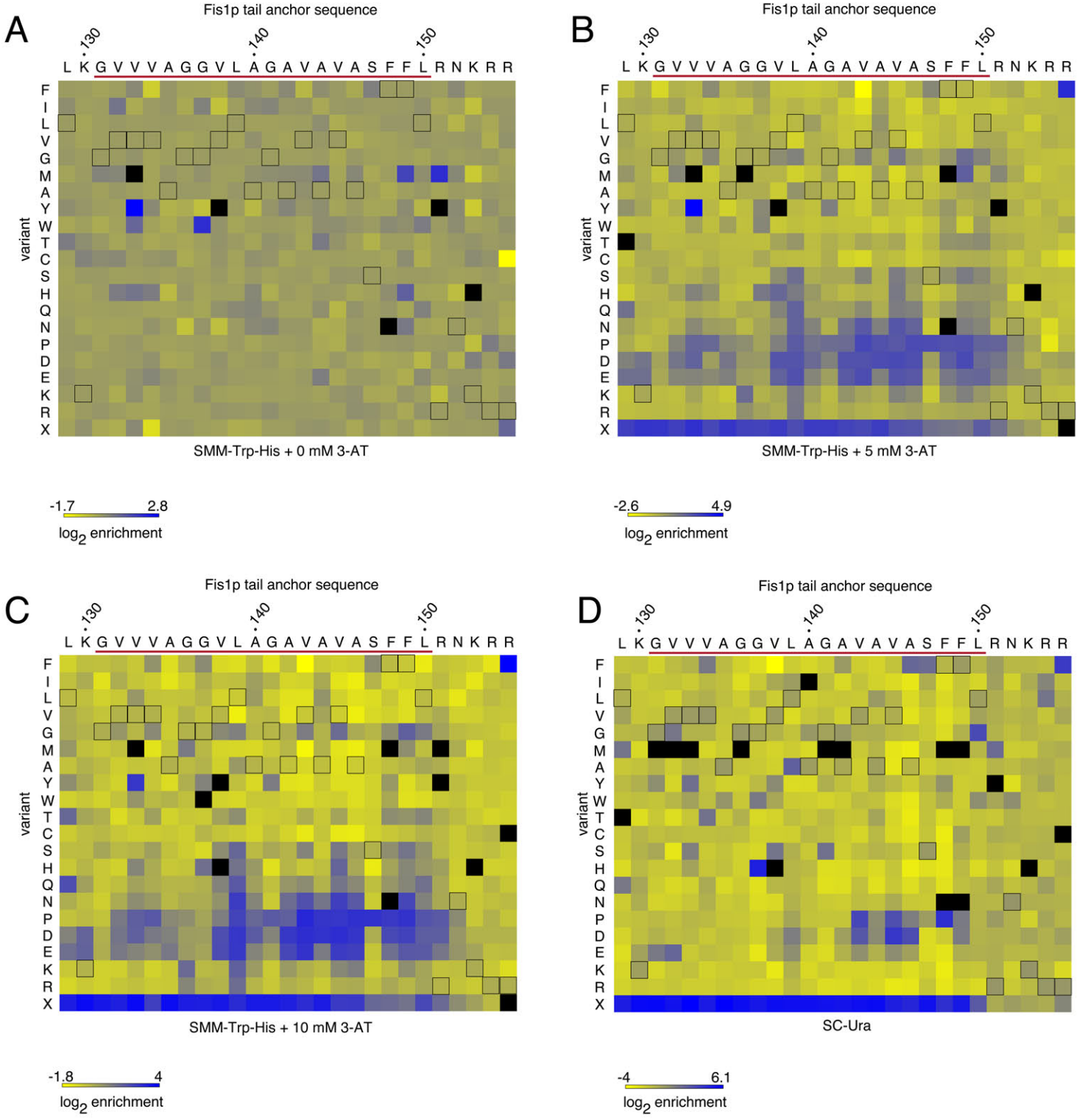

Figure S3

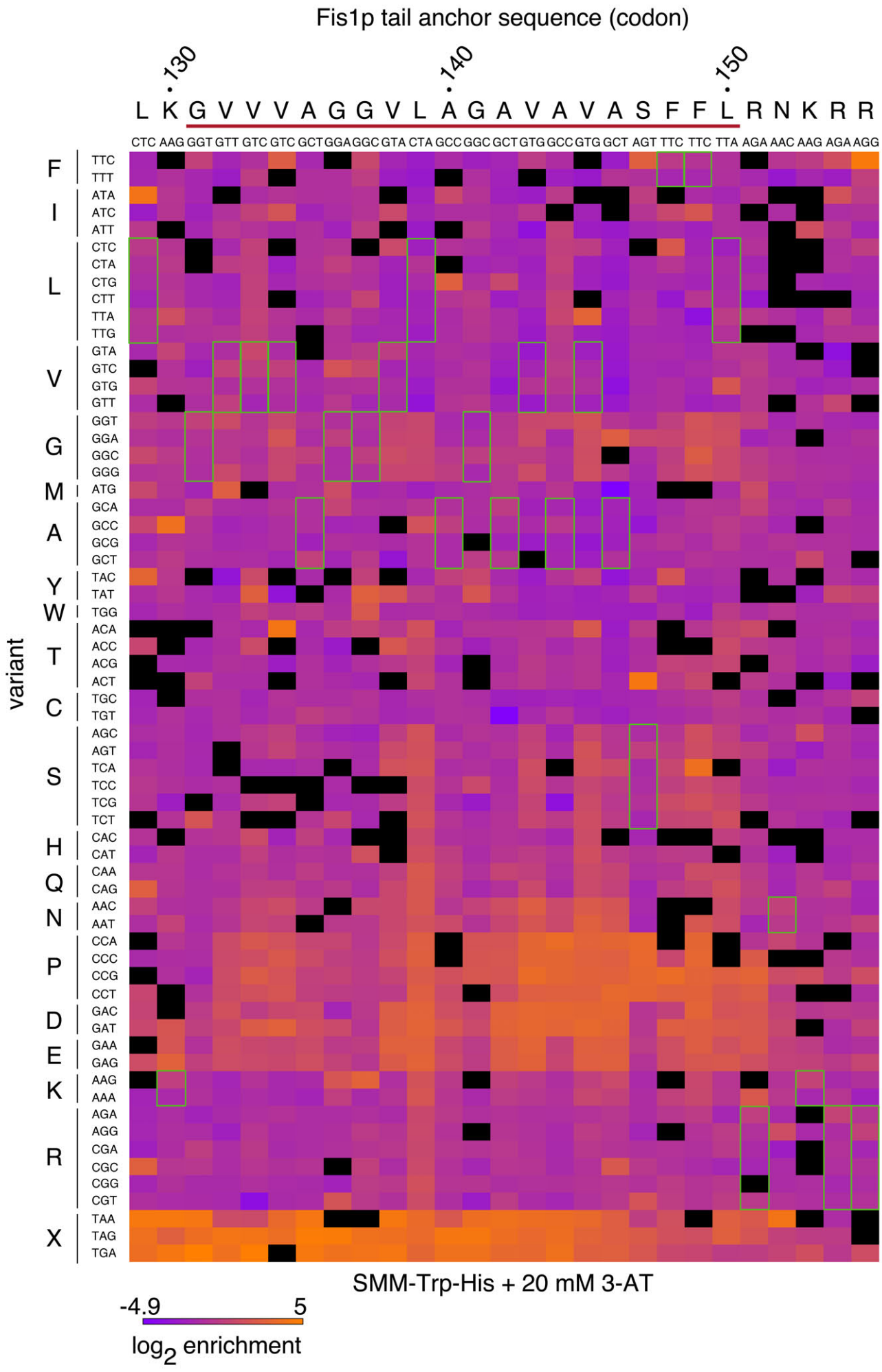

Figure S4

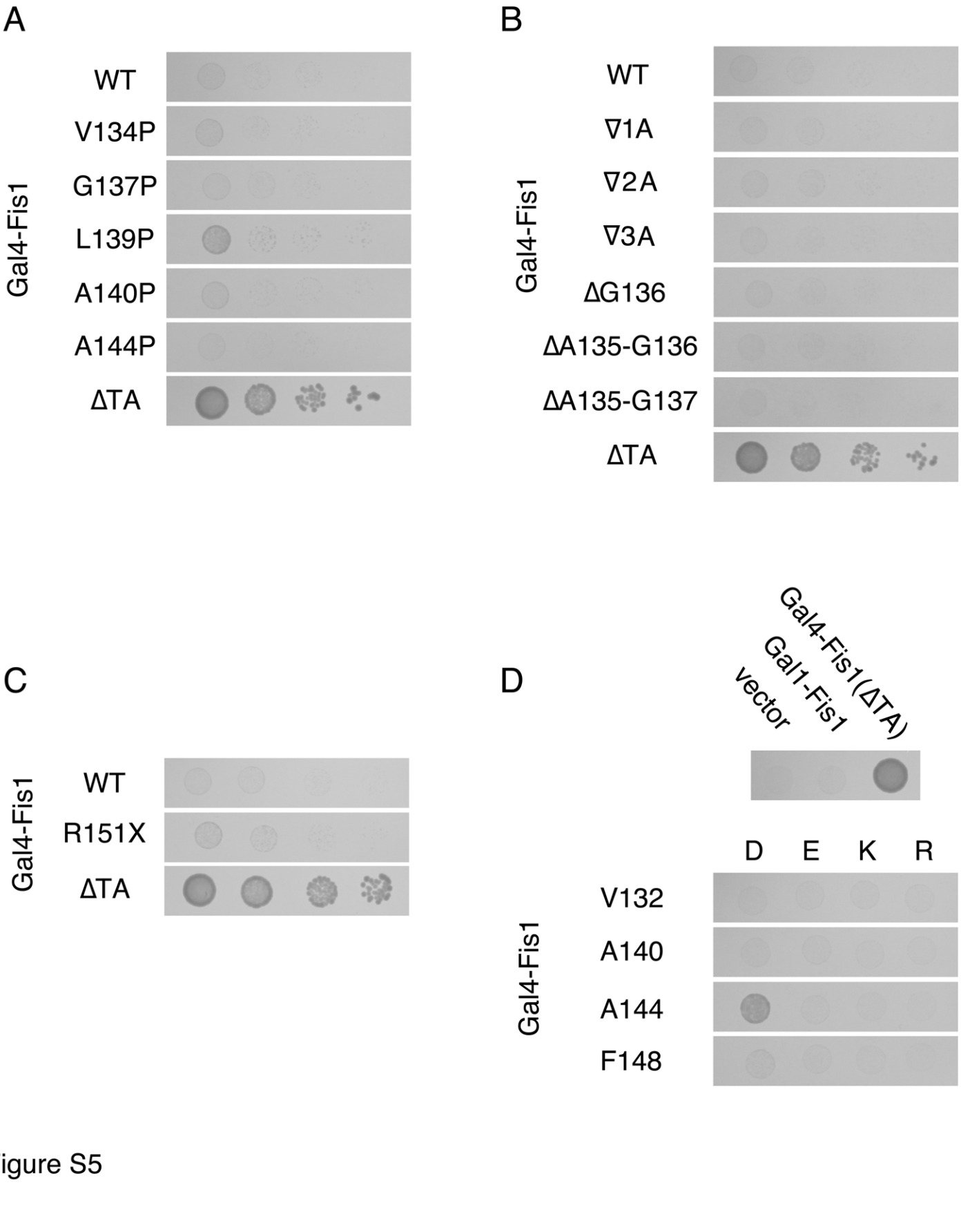

Figure S5

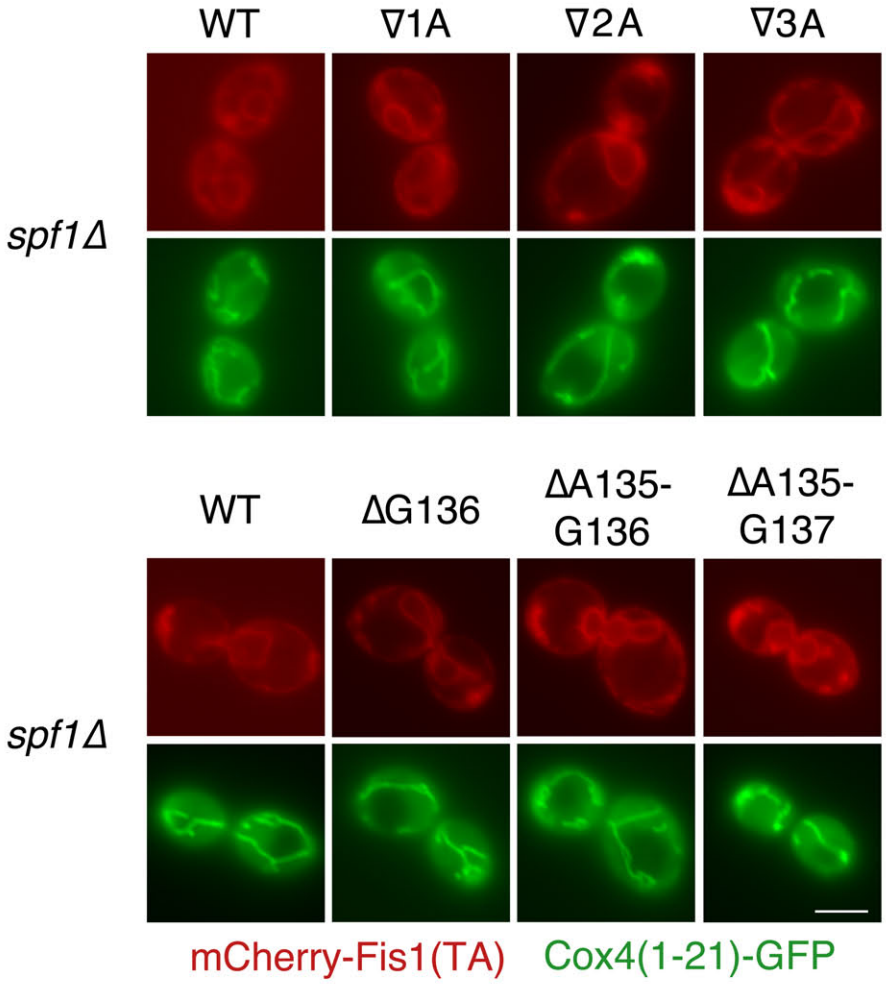

Figure S6

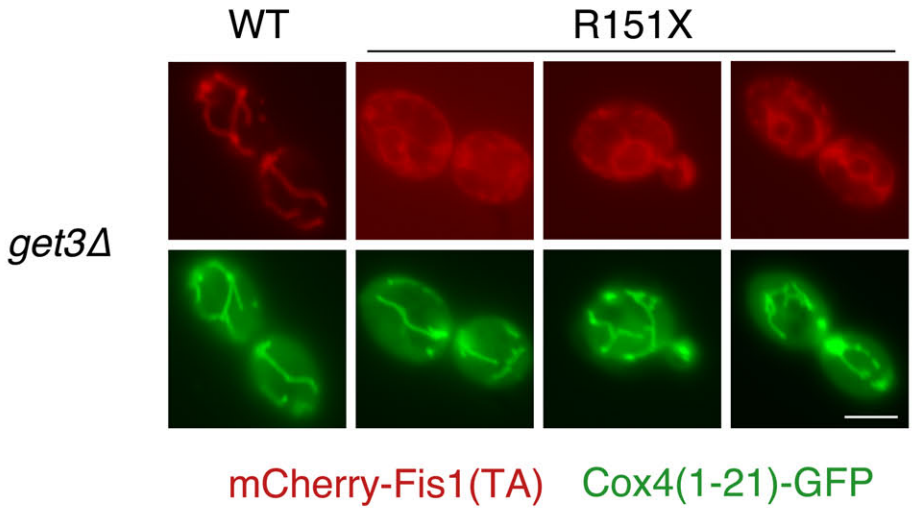

Figure S7

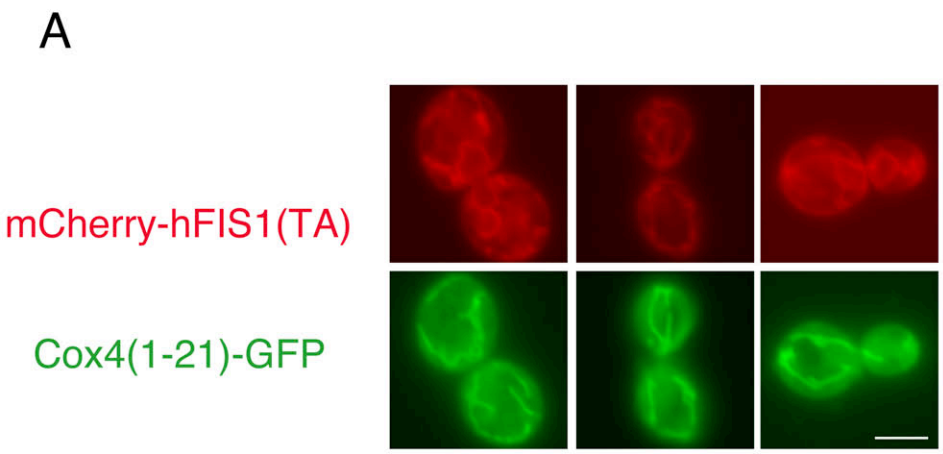

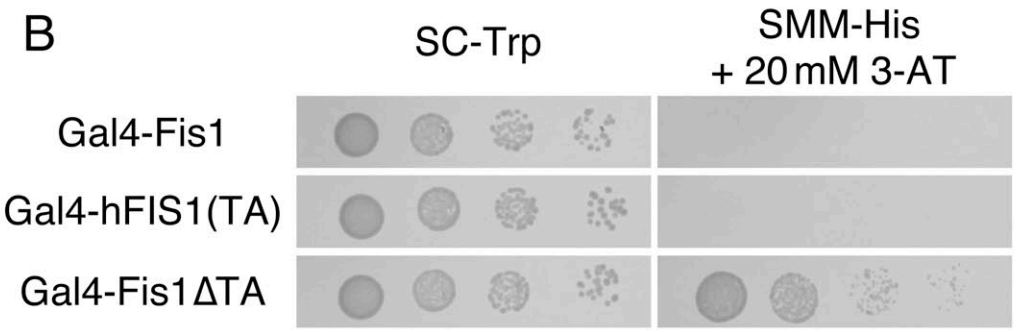

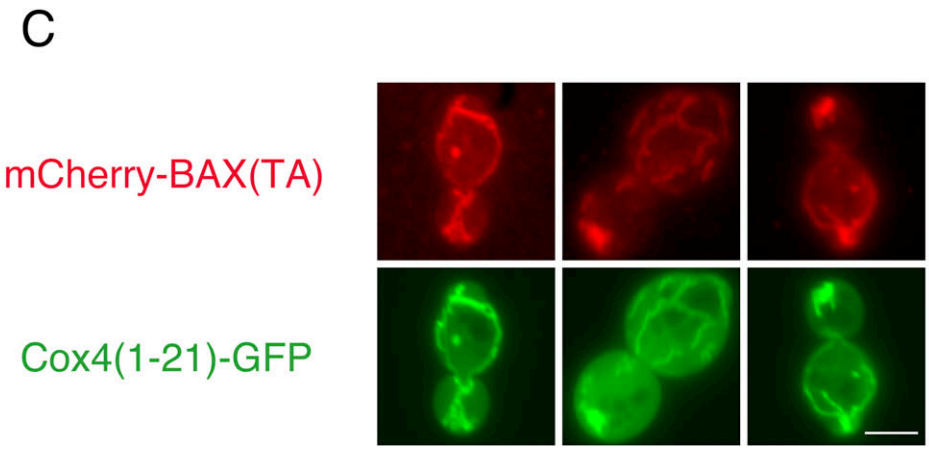

Figure S8

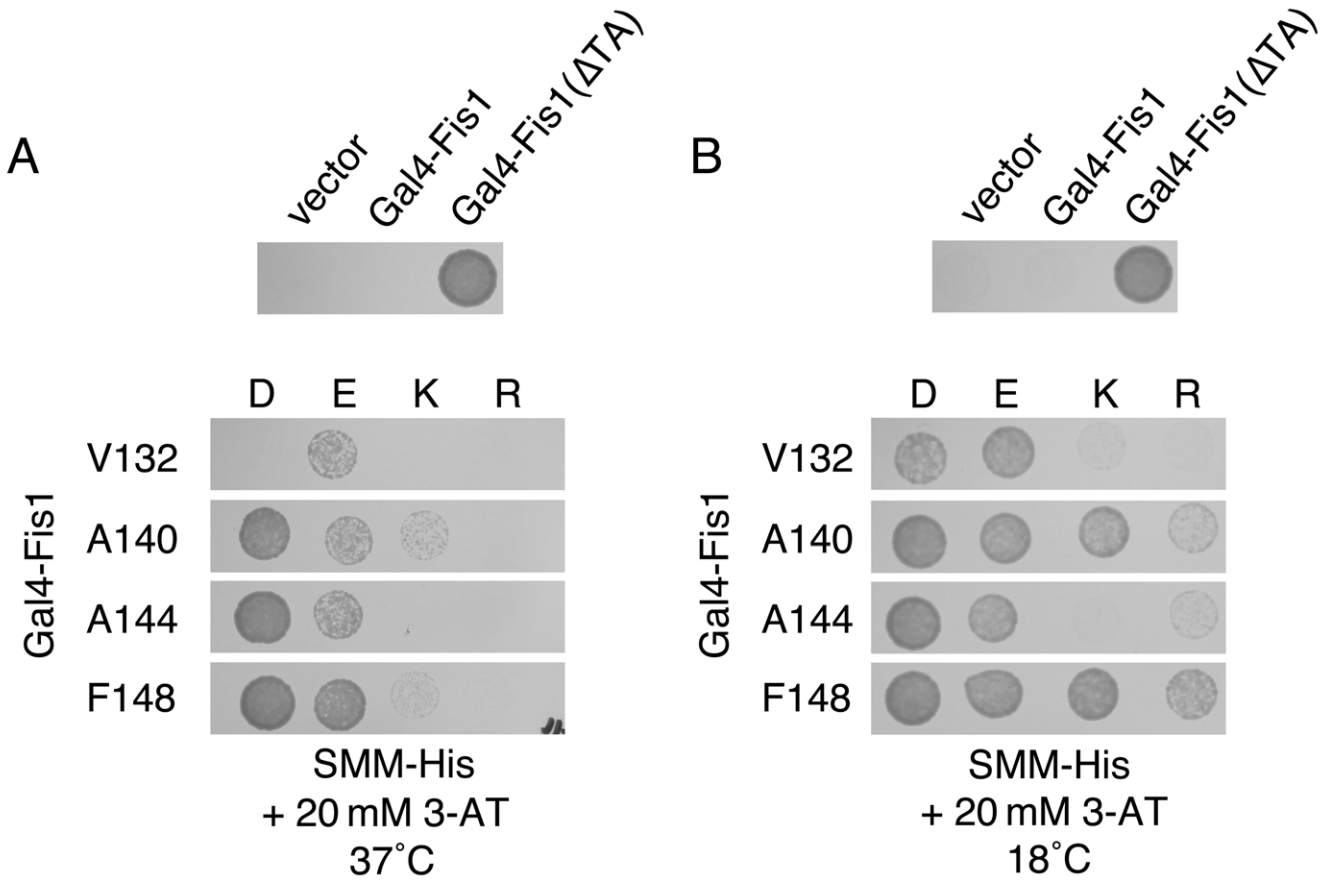

Figure S9

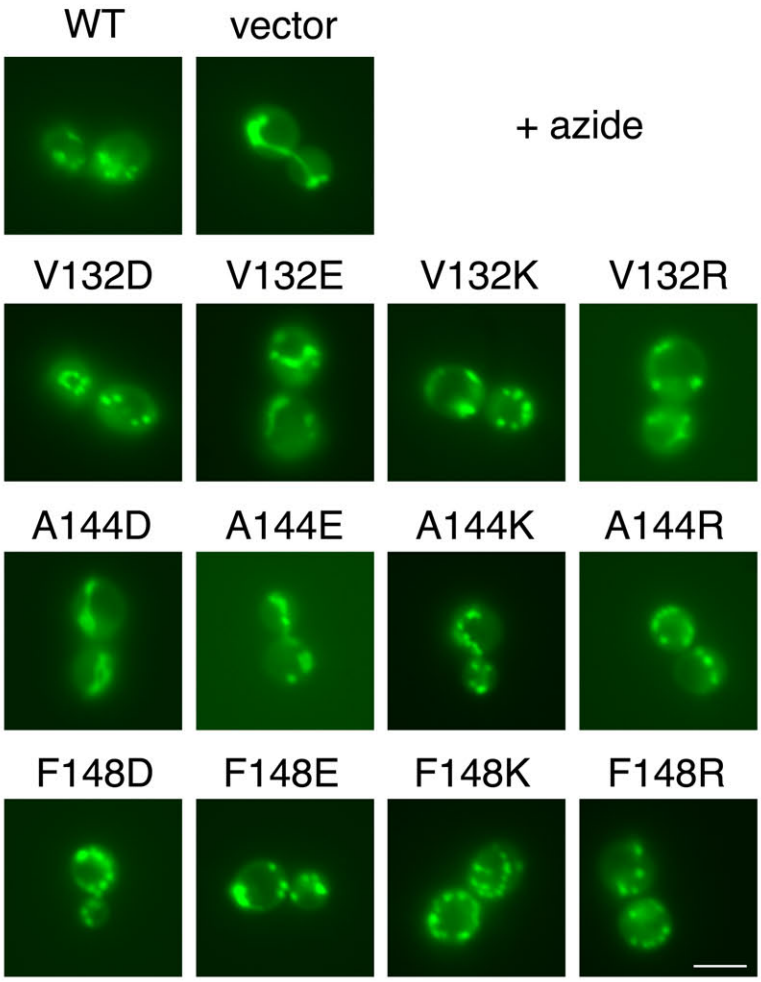

Figure S10